Journal of Thermal Analysis and Calorimetry (2019) 138:1137–1166
https://doi.org/10.1007/s10973-019-08297-3

High-conductivity nanomaterials for enhancing thermal performance of latent heat thermal energy storage systems

Selvaraj Jegadheeswaran[1] · Athimoolam Sundaramahalingam[2] · Sanjay D. Pohekar[3]

Received: 11 September 2018 / Accepted: 26 April 2019 / Published online: 9 May 2019

Abstract
Dispersing high-conductivity nanomaterials into phase change materials (PCM) of latent heat thermal energy storage systems (LHTESS) is expected to solve the problem of poor thermal conductivity of PCMs. Accordingly, several metals, metal oxides and non-metals are employed as nanoadditives for PCMs by researchers. Besides thermal conductivity of PCMs, the other thermo-physical properties are also altered by nanoadditives. This paper provides comprehensive information on the effects of nanoadditives on the thermo-physical properties of PCMs through a critical review of related published works. The modified properties ultimately determine the charging and discharging rates of LHTESS. The extent of improvement in the thermal performance and the related issues are addressed. Further, the theoretical/empirical models developed so far for the evaluation of thermo-physical properties are deliberated.

✉ Selvaraj Jegadheeswaran
jdees.2002@gmail.com

Athimoolam Sundaramahalingam
sundaramahalingama@bitsathy.ac.in

Sanjay D. Pohekar
sdpohekar@gmail.com

[1] Research and Development, Bannari Amman Institute of Technology, Sathyamangalam, Erode (Dt) 638 401, India

[2] Department of Mechanical Engineering, Bannari Amman Institute of Technology, Sathyamangalam, Erode (Dt) 638 401, India

[3] Symbiosis Center for Research and Innovation, Symbiosis International (Deemed University), Lavale, Pune 41211, India

Graphical abstract

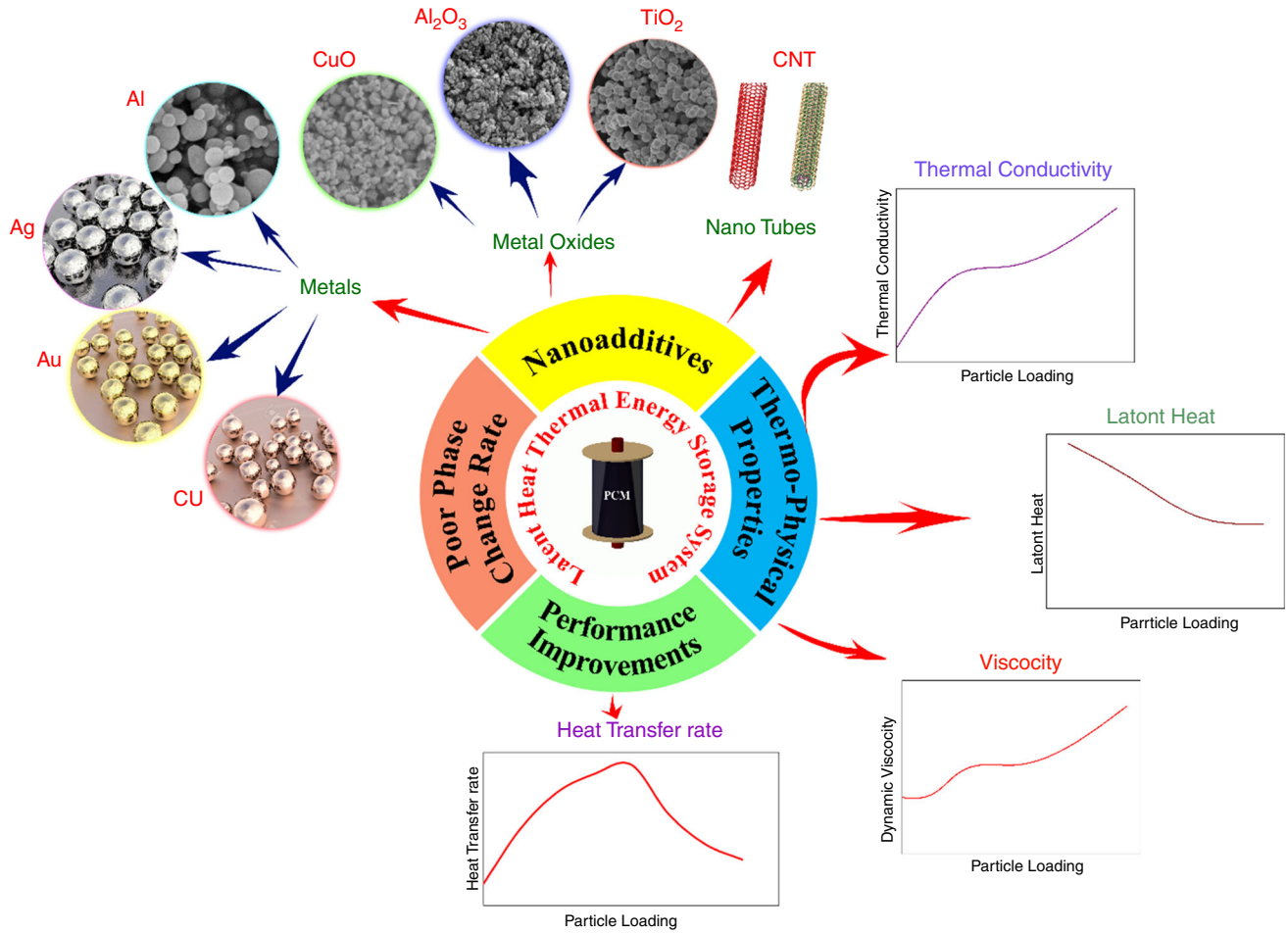

Keywords Energy storage · Phase change material · Heat transfer · Nanomaterial · Brownian motion · Agglomeration

List of symbols

A, B, C, D	Constants in Eq. (14)
B_k	Constant for considering the Kapitza resistance per unit area
B_{2x}	Epolarization factor component along the x-symmetrical axis
Bi	Nanoparticle Biot number
C'	Constant in Eq. (15)
C_1	Proportional constant
C	Specific heat (J kg^{-1} K^{-1})
D_o	Diffusion coefficient
K_B	Boltzmann constant (1.381 × 10^{-23} J K^{-1})
k	Thermal conductivity (W m^{-1} K^{-1})
k_{cx}	Thermal conductivity of complex nanoparticles along x direction (W m^{-1} K^{-1})
k_{cx}	Thermal conductivity of complex nanoparticles along y direction (W m^{-1} K^{-1})
k_l	Thermal conductivity of nanolayer (W m^{-1} K^{-1})
L	Latent heat (J kg^{-1})
l_f	Liquid mean free path
M	Molecular mass
m	Factor in viscosity model of Hosseini et al. [1]
N	Avogadro number
n	Shape function
Pr	Prandtl number
R_b	Interfacial thermal resistance
Re_B	Brownian–Reynolds number
Re_{rp}	Reynolds number based on particle radius
r_c	Cluster radius (m)
r_f	Equivalent radius of a base fluid molecule (m)
r_p	Radius of the particles (m)

T	Temperature (°C or K)
t_{cl}	Thickness of capping layer (m)
t_v	Thickness of the void (m)
V	Velocity (m s^{-1})
X, Y	Constants in Eq. (13)

Greek symbols

α	Volume fraction of base fluid moving with a particle due to Brownian motion, empirical constant in viscosity model of Hosseini et al. [1]
β	Ratio of the nanolayer thickness to the particle radius, empirical constant in viscosity model of Hosseini et al. [1]
γ	Ratio of the thermal conductivity of nanolayer to that of particles, empirical constant in viscosity model of Hosseini et al. [1]
ρ	Density (kg m^{-3})
μ	Viscosity (m^2 s^{-1})
η	Intrinsic viscosity
φ	Volume fraction of nanoparticles
φ_T	Total volume fraction of complex nanoparticles
ψ	Sphericity
τ	Particle relaxation time (s)

Subscripts

eff	Effective
f	Base fluid
l	Nanolayer
max	Maximum
nf	Nanofluid
p	Particle
ref	Reference

Introduction

For the past few decades, scientific community has been trying to address the most serious issues of fossil fuels depletion and greenhouse gases production. The simultaneous solution of these problems remains in the form of renewable energy sources. Among various renewable energy sources, solar energy is given more attention mainly due to its abundant nature. However, even after many years of global research, large-scale utilization of solar energy has not been realized yet as the source availability is inconsistent. This drives the scientific community to look for effective devices to store solar thermal energy. Solar energy storage in the form of latent heat brings out some attractions which include high storage density, isothermal heat transfer, compact modules and availability of storage mediums for wide range of working temperatures.

Despite these favours, the engineering applications of latent heat thermal energy storage systems (LHTESS) are limited predominantly due to the poor thermal conductivity of the storage mediums available. Thus, the storage mediums which are the phase change materials (PCM) are not able to store or release the energy at a reasonable rate. The heat transfer rate can be accelerated by various techniques and the literature reveals few which are,

- Modules with fins
- Use of multiple PCMs
- Thermal conductivity enhancement
- Microencapsulation of PCM

The earlier works on the above techniques are extensively reviewed by Jegadheeswaran and Pohekar [2] and recently Tao and He [3]. Among the techniques, enhancing the thermal conductivity of PCMs using thermal conductivity promoters is simple and straightforward. As described by Fan and Khodadadi [4], there are two classes of promoters: stable structures and free-form enhancers. The high-conductivity stable structures are of different shapes/forms such as fins [5, 6], porous matrices [7], rings [8] and balls [9]. Representative images of those structures are shown in Fig. 1.

As detailed by Jegadheeswaran and Pohekar [2], heat transfer during solidification is majorly by conduction whereas it is by natural convection in liquid PCM during melting except during the initial period. The melting rate may get suppressed as the presence of fixed structures would dampen out the natural convection. Hence, the increase in conduction heat transfer rate due to fixed structures must be much higher so that decrease in convection heat transfer rate would be negligible. This, of course needs careful design of structures and proper form. Further, the volume of structures affects the storage capacity of the system and the porosity of the metals employed plays vital role in altering the latent heat capacity of the PCM. According to Shiina and Inagahi [10], the porosity of metals should be as high as possible for high latent heat capacity. Fan and Khodadadi [4] have reviewed the application of fixed structures as thermal conductivity enhancer for PCMs.

The other option is use of free-moving high-conductivity materials. For long time, researchers have been investigating the augmentation of thermal conductivity of fluids used in heat transfer applications by suspending high-conductivity particles [11]. Conventionally, the dispersed solid additives are of micron sized or sometimes the dimension may be in few millimetres and research on fluids containing such solid particles was started almost 100 years back [12]. In case of PCMs, only few works have reported the employment of micron sized particles. For example,

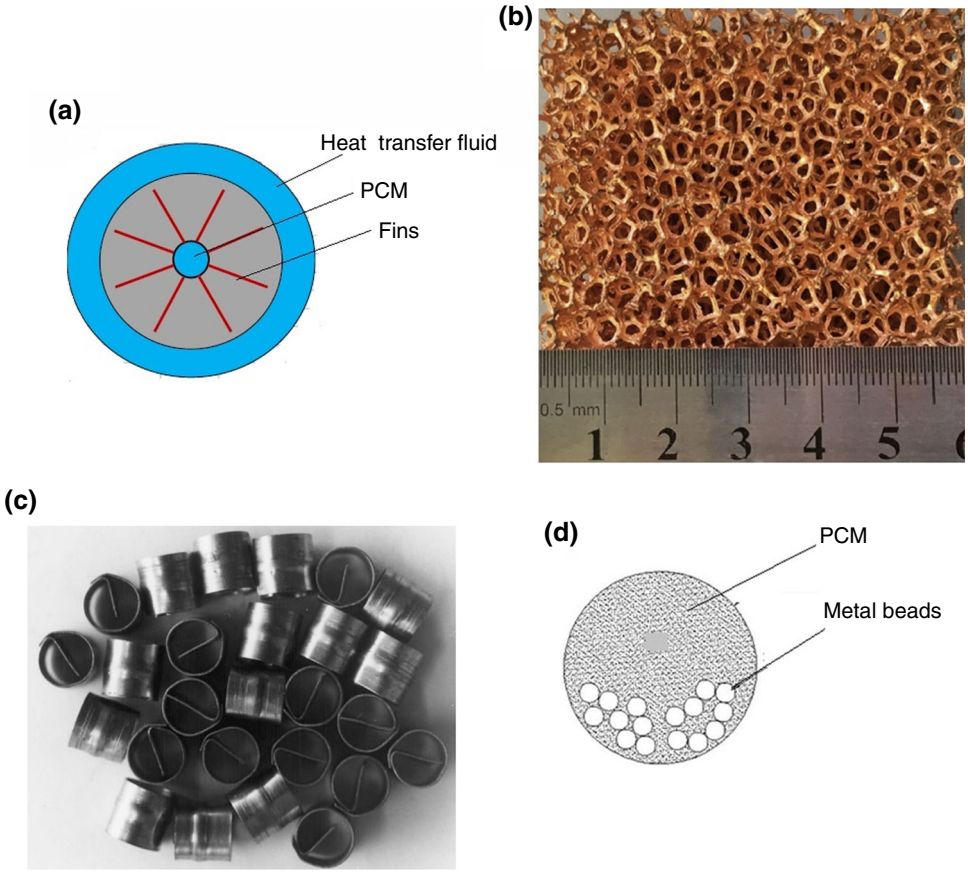

Fig. 1 Fixed thermal conductivity enhancers: **a** fins [5], **b** porous matrices [7], **c** rings [8], **d** balls [9]

Mettawee and Assassa [13] and Chaichan et al. [14] have used aluminium particles and Jegadheeswaran et al. [15] have used copper particles for PCMs. All the authors have reported improved performance; however, the issues of particles settlement are not addressed. In addition to settlement related issues, large size particles may instigate abrasion problem [16]. In this perspective, it can be stated that employing particles of larger size may not be a good idea. Alternatively, materials of various shapes, i.e. particles, fibres, sheets and tubes with average dimension of less than 100 nm have been showing lot of promise in the field of enhanced heat transfer [17]. The nanomaterials are known for inherent attractive features such as high surface area-to-volume ratio, less particle momentum and high particle mobility. Thanks to these features, nanomaterials are expected to offer benefits like higher heat conduction (due to higher surface area), higher microconvection (due to mobility), better stability (due to reduced size) and reduced erosion (due to less momentum) [18]. The nanofluids can be prepared in two methods, namely single step method and two step method [19]. The two preparation methods are outlined in Fig. 2.

In case of heat transfer applications, use of nanomaterials started in the mid-1990s. However, it was limited to mainly fluids of single phase (liquids) and liquid–vapour two-phase fluids until early 2000 [20]. Since then, there has been growing interest among the researchers in nanosize high-conductivity materials added to PCMs. As reported in the earlier works, the nanoadditives can also be used for PCMs to augment the thermal conductivity. Despite good number of works, the full-scale employment of nanoadditives for PCM-based LHTESS needs further research. The relation between altered thermo-physical properties and thermal performance, appropriate material as nanoadditive, optimum concentration of nanoadditives and evaluation of thermo-physical properties are the key issues which need more clarity. In this perspective, this paper is aimed at reviewing the earlier works to present inclusive aspects of nano-PCM research and to identify what to be focussed in future works.

Nanomaterials and thermo-physical properties of composites

Present day nanoscience makes it possible for developing almost all the materials in nanosize. Among the available materials, it is important to choose appropriate materials for PCMs from the perspective that the resulting composites exhibit enhanced thermal performance. However, the

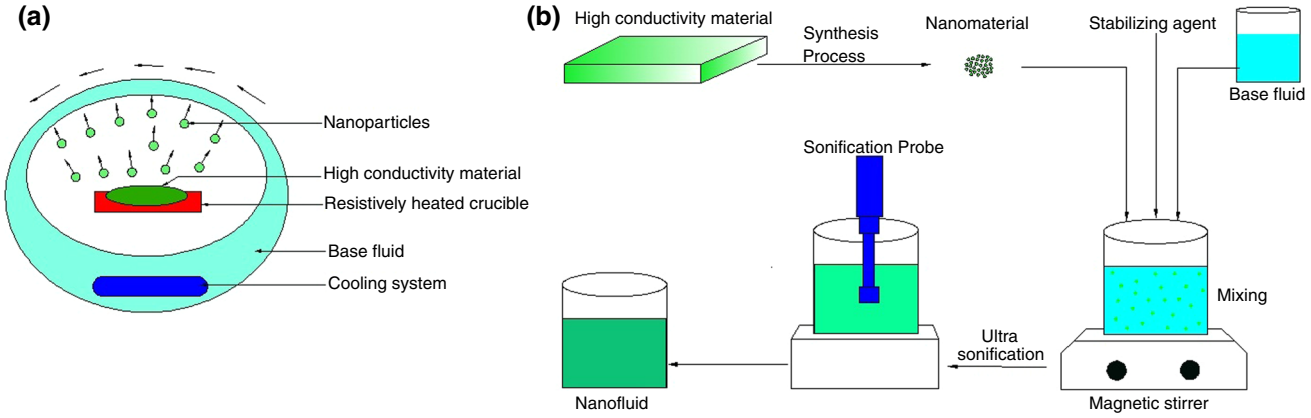

Fig. 2 Nanofluid preparation [19]: **a** single step method, **b** two step method

thermal performance of PCMs depends on the thermo-physical properties and the addition of nanomaterials is expected to alter them. This necessitates the evaluation of thermo-physical properties of composites which would help in great deal in selecting appropriate materials as nanoadditives.

Thermal conductivity of composites

The nanoadditives are used mainly to overcome the poor thermal conductivity of available PCMs. Hence, it is obvious that the material should possess higher thermal conductivity. In this perspective, researchers have identified and employed quite a number of metals and metal oxides. Further, few non-metals are also in the picture. The list of various materials employed as nanoadditives with their thermal conductivity values is given in Table 1.

Among metals, copper is widely employed as it is superior in terms of thermal conductivity. Lin and Al-kayiem [28] have shown that paraffin wax's thermal conductivity could be increased by 30% with copper nanoparticles of 2% volume fraction. Zeng et al. [29] have used copper particles for tetradecanol and have reported 9 times higher thermal conductivity when 12% volume of copper nanowires was dispersed. Khodadadi and Hosseinzadeh [30], Hosseinzadeh et al. [21] and Sebti et al. [31] have not measured the thermal conductivity of nanocopper–PCM composites as these are basically numerical studies. However, these works reveal that the charging and discharging rates of composite PCMs are quite higher as compared to those of pure PCM. It is obvious that higher phase change rates are because of enhanced thermal conductivity. Hence, copper nanoadditives seem to be a potential candidate for enhancing the phase change rate. Apart from copper, aluminium and silver have also been utilized. For example, Constantinescu et al. [32] and Kalaiselvam et al. [33] have used aluminium and Wei [23], Parameshwaran et al. [34] and Zeng et al. [35] have used silver. The results are interesting as Parameshwaran et al. [34] could achieve 67% increase in thermal conductivity of organic ester with 5% mass fraction of silver particles.

Table 1 List of nanomaterials with their thermal conductivities

Material	Thermal conductivity of bulk material/ W m^{-1} K^{-1}	References
Copper	400	Hosseinizadeh et al. [21]
Aluminium	237	Michaelides [22]
Silver	427	Wei [23]
CuO	18	Abolghasemi et al. [24]
Alumina	36	Elbahjaoui et al. [25]
TiO_2	8.9538	Naeem et al. [26]
SiO_2	1.5	Manoj Kumar and Maylsamy [27]
Carbon nanotubes	3200	Michaelides [22]

The most tested metal oxides as nanoadditives for PCMs are copper oxide, aluminium oxide (alumina) and titanium oxide. All these metal oxides are also proven to be good thermal conductivity enhancers. Harikrishnan and Kalaiselvam [36] employed oleic acid with copper oxide. The increase in thermal conductivity was up to 100% when 2% (mass fraction) particles were dispersed. However, Jesumathy et al. [37] have given contradictory results as even 10% mass fraction of copper oxide could result in an increase of only 7.8%. In case of alumina, mass fraction of 10% could improve the thermal conductivity of paraffin by 17% [38]. Similarly, $BaCl_2$ solution ended with 16.74% improvement due to titanium oxide of 1.13% volume fraction [39]. The above outcomes indicate that the metal oxides can also work well for PCMs. However, TiO_2 is found to be superior to other metal oxides by Teng and Yu

[40]. The superiority of TiO_2 over alumina is also demonstrated by Raja Jeyaseelan et al. [41]. Moreover, due to better suspension stability, TiO_2 could widen up the phase change range of paraffin. This allows melting process to occur even with relatively low temperature heat source.

The summarized studies indicate that all metal oxides are far inferior as compared to metals. This is because metals generally possess excellent thermal conductivity than their respective oxides, and one can come to the conclusion that metals are better choice than metal oxides. However, metals tend to oxidize which in turn reduces the thermal conductivity of PCMs over a period of time. Moreover, the metal additives would increase the mass and cost of the storage systems considerably. Hence, it is important to look for effective materials as nanoadditives other than metals and metal oxides.

Accordingly, nanoversions of carbon and its allotrope graphite are found to be potential candidates as carbon possesses low density compared to metals but comparable thermal conductivity. Kibria et al. [42] have indicated that carbon and graphite materials also possess some unique properties like resistance to corrosion/chemical attack and compatibility with all PCMs. In case of graphite, investigators have largely employed exfoliated graphite nanoplatelets (xGnP) although graphite nanofibres and graphene are also found to be suitable [43]. Shi et al. [44] have revealed the ineffectiveness of graphene due to more number of nanointerfaces which result in high interfacial thermal resistance, and hence, xGnP is suggested for effective thermal conductivity enhancement. At the same time, graphene would significantly enhance the shape stabilization performance due to its higher specific surface area than xGnP. Hence, the authors have suggested employing both the materials at right proportion but in smaller fraction. Kim and Drzal [45] have used xGnP up to 7% mass fraction for improving thermal conductivity of paraffin and have reported more than 200% increase. Jeon et al. [46] investigated the benefit of adding xGnP into three types of PCMs namely octadecane, heaxadecane and paraffin. All the composites showed remarkable results with a maximum of 100% when 5% mass fraction of xGnP was added into octadecane. However, Li [47] recently has claimed that nanographite powder has larger specific surface area and length–diameter ratio than xGnP and thus can form heat transfer network. Accordingly, the thermal conductivity of paraffin is increased by 250% with 7% mass fraction of nanographite powder as against 200% increase reported by Kim and Drzal [45]. The works discussed above highlight a near linear increase in PCMs' thermal conductivity with graphite loading.

Carbon is another widely employed nanoadditives for PCMs in various forms. The use of carbon as nanoadditives for PCM was initiated by Elgafy and Lafdi [48] by employing carbon nanofibres (CNF) for paraffin wax. The thermal conductivity was improved by around 35% with 4% mass fraction of CNF. In another work by Sakalaukus et al. [49], the paraffin wax conductivity was observed to be increased by about 40% when 4% mass fraction of CNF was used.

However, the current research on nanomaterials takes special interest in carbon nanotubes (CNT). CNF with graphene layers wrapped into perfect cylinders are called CNTs for which extremely high thermal conductivity is predicted [50]. The high thermal conductivity is the result of large photon mean free path [51]. The CNTs can be either single walled (SWCNT) or multi-walled (MWCNT). The schematic representation of the structure of SWCNT and MWCNT is presented in Fig. 3. In general, CNTs possess very high thermal conductivity, i.e. fivefolds as compared to copper.

Using 0.6% volume fraction of MWCNT, Kumaresan et al. [52] could augment the thermal conductivity of paraffin by around 45%. Similarly, Wang et al. [53] have reported 30% higher thermal conductivity for palmite acid due to the addition of 1% mass fraction of MWCNT. The above-mentioned works have observed linear enhancement with CNT in both solid and liquid states. However, according to Lajvardi et al. [54], thermal conductivity of PCM has only nonlinear increase with MWCNT loading. Ji et al. [55] have recommended functionalized MWCNTs (oxidized MWCNTs adsorbed pyrogallol) for better thermal conductivity enhancement as this class has better dispersing capability than oxidized MWCNTs. On the other hand, Wu et al. [56] have suggested employing nanoencapsulated PCMs which are formed by impregnating PCMs in CNTs in place of nanocomposite PCMs. The authors have reported that the thermal conductivity of lauric acid could be increased by more than 20 times when the PCM was nanoencapsulated. Among carbon additives, graphite powder is preferred as it exhibits higher thermal conductivity enhancement than CNT and is also less expensive [57].

Besides non-metals, oxides of non-metals have also been studied as nanoadditives for PCMs. Selvaraj et al. [58] have shown thermal conductivity increase as 39% and 15% for deionized water and ethylene glycol, respectively, with 2% volume fraction of beryllium oxide (BeO). On the other hand, Manoj Kumar and Mylsamy [27] employed silicon oxide (SiO_2) for paraffin wax and have reported around 23% enhancement in thermal conductivity with 1% mass fraction although effect of volume fraction of nanoadditives was not investigated.

The concluded discussion clearly indicates that all the tested nanoadditives are capable of enhancing the thermal conductivity of various PCMs. Table 2 presents the role of

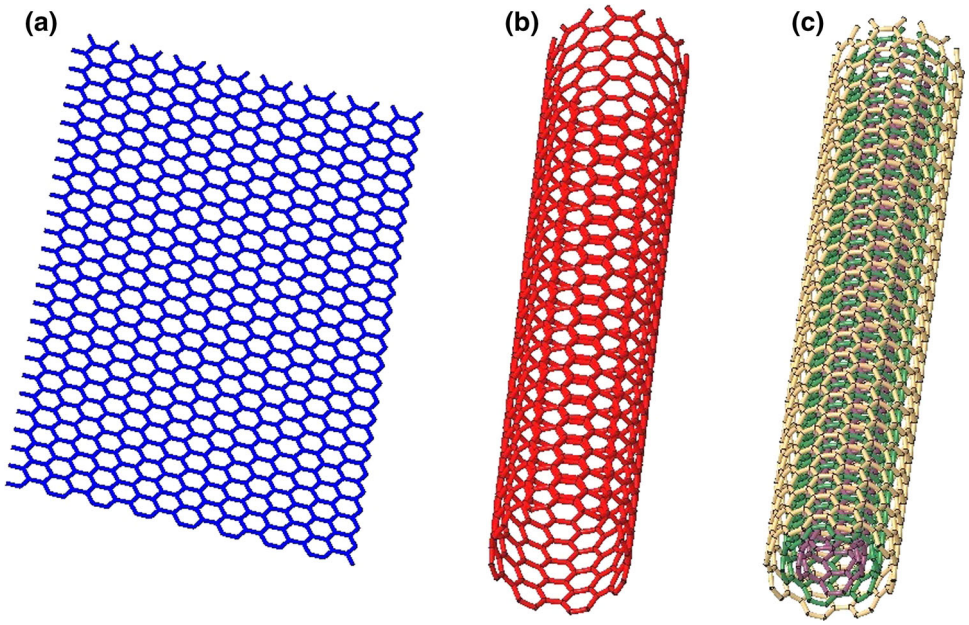

Fig. 3 Structure of carbon nanotubes (CNT) [50]: **a** graphite lattice, **b** single walled CNT, **c** multi-walled CNT

different classes of nanomaterials in enhancing thermal conductivity of various PCMs. However, the increase is generally nonlinear with increase in concentration of nanoadditives which is shown in Fig. 4.

At this point, it is also imperative to address the consequence of particle size as far as thermal conductivity enhancement is concerned. To investigate the same, Zabalegui et al. [68] carried out experimental study on multi-walled carbon nanotube (MWNT) added to paraffin. Although the particle diameter is found to have negligible role, there are good number of works show the other way. According to Keblinski et al. [69], the mixture thermal conductivity is a function of not only particle volume fraction but also of particle size. Eastman et al. [70] have shown the inadequacy in calculation of thermal conductivity of nanofluids if only the concentration and shape of particles are taken into account. The need for comprehensive studies with samples of varying particle size with same composition is also stressed by the authors. Masuda et al. [71] have found 30% increase in thermal conductivity of water using Al_2O_3 nanoparticles of 4.3 vol% which has a mean diameter of 13 nm. On the other hand, Lee et al. [72] observed less than 10% enhancement only with same Al_2O_3 nanoparticle but of mean diameter of 38 nm. This indicates that decrease in particle size leads to increase in thermal conductivity. On the contrary, the increase in particle diameter of MWCNT resulted in increase in thermal conductivity of paraffin wax as reported by Temel et al. [73]. The authors have attributed this to the effective photon transfer due to larger particle size.

The relationship between particle size and thermal conductivity is due to Brownian-induced motion of the nanoparticles. Significant number of works focusing on the Brownian motion can be found in the literature [74–79]. Prasher et al. [80] have demonstrated that the Brownian motion is the prime contributor to the thermal conductivity enhancement. The Brownian motion is nothing but the irregular movement of the particles caused by the random collisions of the surrounding liquid molecules [81]. Figure 5 presents the schematic of Brownian motion of a particle.

Since nanoparticles possess surface energy due to higher surface area, the Brownian motion gets accelerated which in turn makes it nanoconvection dominant [53]. To quantify Brownian motion, the time averaged velocity of the particles (thermophoretic velocity) under a steady temperature gradient is calculated. Michaelides [22] has stated that the thermophoretic velocity depends on particle size. According to the order-of-magnitude analysis presented by Prasher et al. [80], the Brownian motion of smaller particles is stronger than that of relatively bigger particles. This shows that maximum benefit can be achieved if particles of least possible diameter are used. However, Shin and Banerjee [82] have stressed that the interfacial thermal resistance between particles and base fluid increases with decrease in particle size and thus improved thermal conductivity with particles of smaller size. Hence, the optimum size of the particles should be known to extract maximum benefit in terms of higher thermal conductivity. The optimum size can be estimated using the values of interfacial thermal resistance and thermal conductivities of base fluid and nanoparticles. The required expression can be found in the articles of Prasher et al. [80] and Shin and Banerjee [82]. The list of past works which have reported

Table 2 Role of various nanomaterials in thermal conductivity enhancement of PCMs

References	PCM	Nanomaterial	Concentration of nanomaterial employed	Thermal conductivity enhancement
Arasu et al. [59]	Paraffin wax	Al_2O_3	2, 5 and 10 vol%	About 30%
Arasu et al. [60]	Paraffin wax	Al_2O_3 and CuO	0–10 vol%	About 30% at 27 °C and the enhancement increases with temperature
Elgafy and Lafdi [48]	Paraffin wax	CNF	1, 2, 3 and 4 mass%	About 35%
Fan and Khodadadi [61]	Cyclohexane (C_6H_{12})	CuO	1, 2 and 4 mass%	About 5%
Fang et al. [62]	Paraffin wax	Hexagonal boron nitrode (h-BN) sheets	1–10 mass%	Up to 60%
Harikrishnan and Kalaiselvan [63]	Oleic acid	CuO	0.5, 1.0, 1.5 and 2.0 mass%	Up to 98.66%
He et al. [39]	Saturated $BaCl_2$ aqueous solution	TiO_2	0.167, 0.283, 0.565 and 1.13 vol%	Up to 16.67%
Jesumathy et al. [37]	Paraffin wax	CuO	2, 5 and 10 mass%	3.77%, 6.92% and 13.21%, respectively
Ji et al. [55]	Palmitic acid	Functionalized MWCNT	1, 2, 3, 5 and 7 mass%	About 60%
Lin and Al-kayiem [28]	Paraffin wax	Cu	1 and 2 mass%	12.24% and 31.29%, respectively
Motahar et al. [64]	*n*-Octadecane	Mesoporous silica ($MPSiO_2$)	1, 3 and 5 mass%	6%
Parlak et al. [65]	Paraffin wax	MWCNTs (short and long)	1, 3 and 5 mass%	8.4% and 33.7% for short and long MWCNTs, respectively
Nabhan [66]	Paraffin wax	TiO_2	1, 3 and 5 mass%	About 10%
Khodadi and Hosseinizadeh [30]	Water	Cu	0–0.2 vol%	74.5%
Parameshwaran et al. [34]	Organic ester	Ag	0.1–5 mass%	10–67%
Ho and Gao [38]	*n*-Octadecane	Al_2O_3	5 and 10 mass%	6% and 17% at 30 °C and 60 °C, respectively
Sakalaukus et al. [49]	Paraffin wax	CNF	4 mass%	40%
Sebti et al. [31]	Paraffin wax	Cu	0.025 and 0.05 vol%	7.64% and 1.75%, respectively
Shi et al. [44]	Paraffin wax	xGnP and Graphene	1, 2, 5 and 10 mass%	XGnP shows greater thermal conductivity improvement than graphene, and with 10 mass%, thermal conductivity is increased tenfold for xGnP
Teng and Yu [67]	Paraffin wax	Al_2O_3, TiO_2, SiO_2 and ZnO	1, 2 and 3 mass%	TiO_2 is superior than others in enhancing thermal conductivity
Zeng et al. [35]	Tetradecanol (TD)	Ag	1:64 to 16:1	Thermal conductivity increases with Ag loading
Zeng et al. [29]	Tetradecanol (TD)	Cu nanowires	0–11.9 vol%	Thermal conductivity increases with particle loading, and after 1.5 vol% the thermal conductivity increases very rapidly. It attains nine times higher thermal conductivity at 11.9 vol%
Kim and Drzal [45]	Paraffin wax	xGnP	1, 2, 3, 5 and 7 mass%	2 times
Kumaresan et al. [52]	Paraffin RT-20	MWCNT	0.15, 0.3, 0.45 and 0.6 mass%	40–50% for 0.6 mass%
Lajvardi et al. [54]	Paraffin wax emulsion (paraffin 2 mass%)	MWCNT	0.2, 1 and 2 vol%	About 31% near melting point
Li [47]	Paraffin wax	Nano-graphite	1, 4, 7 and 10 mass%	7.41 times
Wang et al. [53]	Palmitic acid	MWCNT	0.2, 0.5 and 1 mass%	About 45% and 35% in solid state and liquid states, respectively

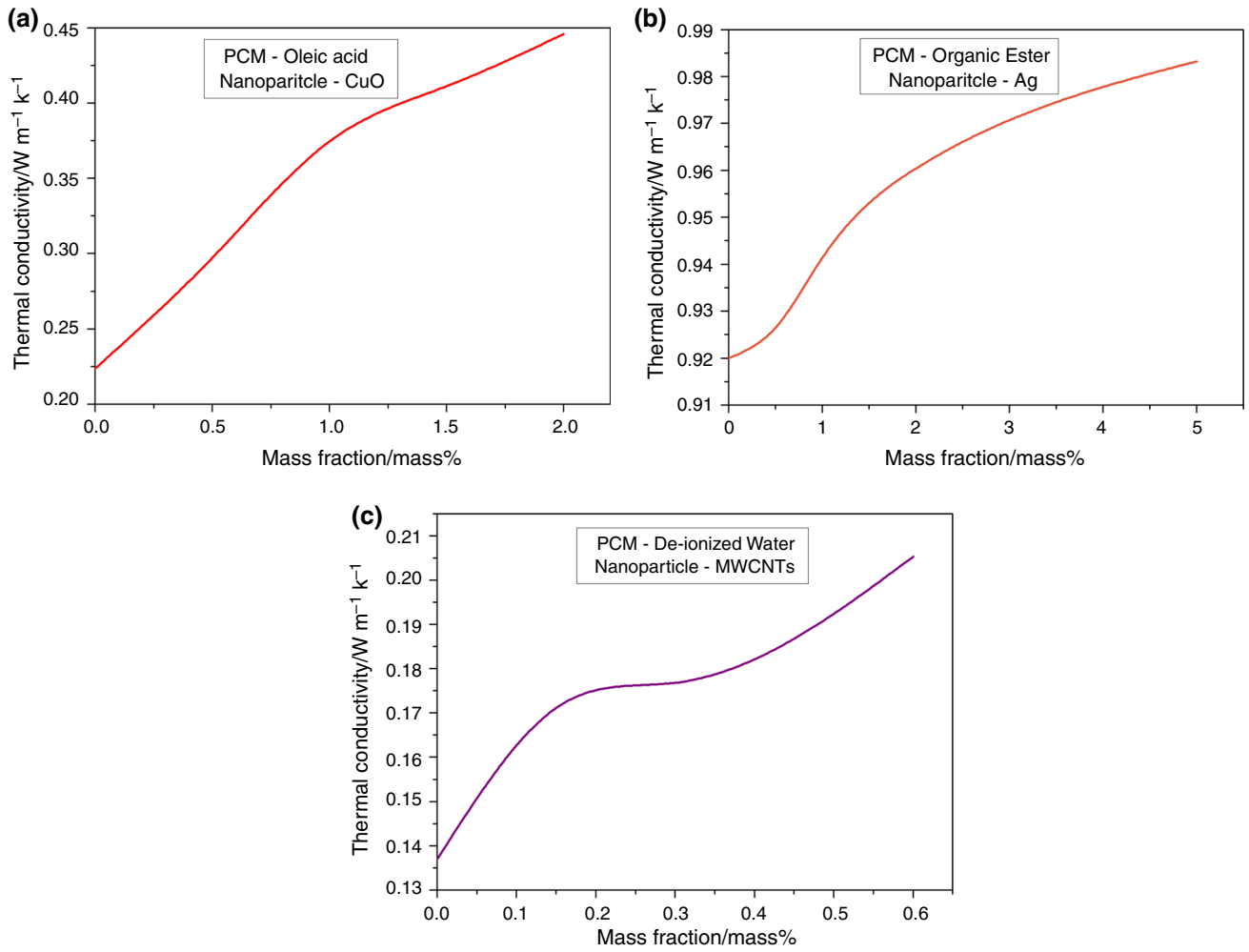

Fig. 4 Nonlinear variation of thermal conductivity with particle loading: **a** CuO [36], **b** Ag [34], **c** CNT [52]

the relationship between particle size and thermal conductivity is presented in Table 3.

Latent heat of composites

It is a matter of concern as the addition of nanomaterials may lead to reduction in latent heat value of PCM. According to Cai et al. [85] who prepared paraffin with high density polyethylene (HDPE), the additive in the composites makes the three-dimensional net structure more compact which reduces the molecular heat movement of PCM. Since the authors have not used nanoadditives, the validity of above phenomenon is not clear when it comes to nanoadditives-dispersed PCMs.

Latent heat value of PCMs is the direct measure of storage capacity of LHTESS modules. If the addition of nanomaterials results in significant reduction in latent heat of PCM, then the energy density of the storage unit would not be up to the mark. This makes no sense in employing PCM-based LHTESS units even if there is a drastic improvement in heat transfer. The reduction in latent heat due to metal nanoadditives is addressed by Parameshwaran et al. [34] and Zeng et al. [29]. Parameshwaran et al. [34] observed that addition of silver nanoparticles (5 mass%) into organic ester resulted in 11% decrease in the latent heat. On the other hand, 7.42% mass of copper nanoparticles led to reduction of latent heat of tetradecanol by 9.4% as reported by Zeng et al. [29].

The nanoversions of metal oxides are also found to be behaving like metals in reducing the latent heat. For example, 2% mass fraction of CuO led to a reduction in latent heat of oleic acid by 5.2% according to Harikrishnan and Kalaiselvam [36]. He et al. [39] have shown that 1.13% volume fraction of TiO_2 resulted in 9.5% reduction of latent heat of $BaCl_2$ solution, whereas 4% reduction for paraffin wax is reported by Nabhan [66] with 5% mass fraction of TiO_2. Similarly, addition of 5% and 10% mass fraction of Al_2O_3 resulted in 7% and 13% reduction, respectively, for the latent heat of paraffin according to Ho and Gao [38]. However, Saeed et al. [86] could observe the

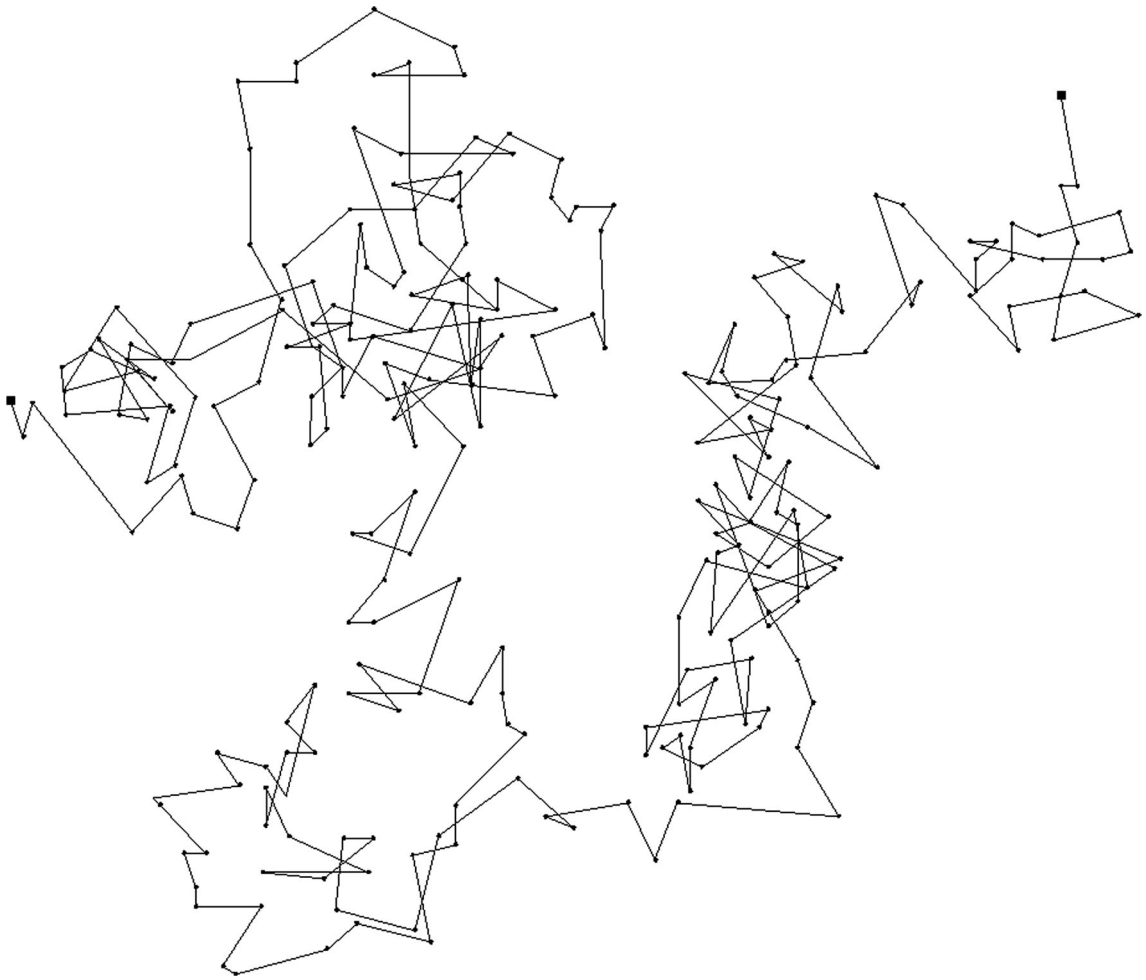

Fig. 5 Brownian motion of a particle

Table 3 Summary of works investigated the effect of particle size on effective thermal conductivity

References	Nanomaterial	Range of particle size	Nature of work	Highlights
Eastman et al. [70]	Ethylene Glycol	< 10 nm	Experimental	Theoretical models which consider only volume fraction and particle shape and ignoring particle size are insufficient
				Inaccuracy in the results due to non-inclusion of particle size is more pronounced in metal-based nanofluids than metal oxides
Prasher et al. [83]	–	–	Analytical	Convection due to Brownian motion is responsible for enhancement in thermal conductivity
				Brownian motion-based convective–conductive model accurately captures the effect of particle size.
Shin and Banerjee [82]	SiO_2	2 nm	Analytical	Molecular dynamics simulation is performed
				Interfacial thermal resistance increases with decrease in particle size
				Optimum diameter is found to be 10 nm
Zabalegui et al. [68]	MWCNT	15.5 nm, 40 nm, 65 nm and 400 nm	Experimental	Particle diameter has significant effect on latent heat but negligible influence on thermal conductivity
Zabalegui et al. [84]	MWCNT	15.5 nm, 40 nm, 65 nm and 400 nm	Experimental	With smaller particles, the enhancement in thermal conductivity is not significant enough to overcome the reduction in latent heat, and thus less energy is stored

reduction only when mass fraction of Fe_3O_4 was 5% and above though there was slight improvement with 1 mass%.

Like metals and metal oxides, the non-metallic additives are found to be causing the reduction in latent heat. Li [47] has observed a maximum of 10% reduction in latent heat of paraffin with 10% mass fraction of graphite, whereas 3% mass fraction of CNT brings down the same by 3.69% [67, 87]. The MWCNT used by Parlak et al. [65] prompted less than 10% of reduction when the mass fraction was 5%. Similar effect is also observed by Kumaresan et al. [52] and Xiang and Drzal [88] with MWCNT and xGnP, respectively. Fang et al. [62] have used boron nitride nanosheets for paraffin and have found latent heat reduction of less than 12% even with 10% mass fraction of nanoadditives against the maximum thermal conductivity enhancement of 60%.

Contrary to all the above works, the results of Chieruzzi et al. [89] show an increase in latent heat due to nanoadditives. In spite of this, the above summary affirms that all types of nanoadditives cause reduction in latent heat in all cases (Fig. 6). However, considering the extent to which the thermal conductivity is enhanced, the reduction in latent heat is less significant. The same can be confirmed from the results of Risueno et al. [90] as the change in latent heat values of PCMs was found to be less significant when metal alloys were used as nanoadditives. Nevertheless, the quantity of nanoadditives should be kept as minimum as possible to minimize the adverse effect on latent heat.

Besides the concentration of nanoadditives, the size also has a role in altering latent heat. Shaikh and Lafdi [91] have used SWCNT, MWCNT and CNF in paraffin wax and have shown that SWCNT which was the smallest among the three caused higher enhancement in latent heat. Accordingly, the authors have stated that the smaller size particles having higher molecular density would increase

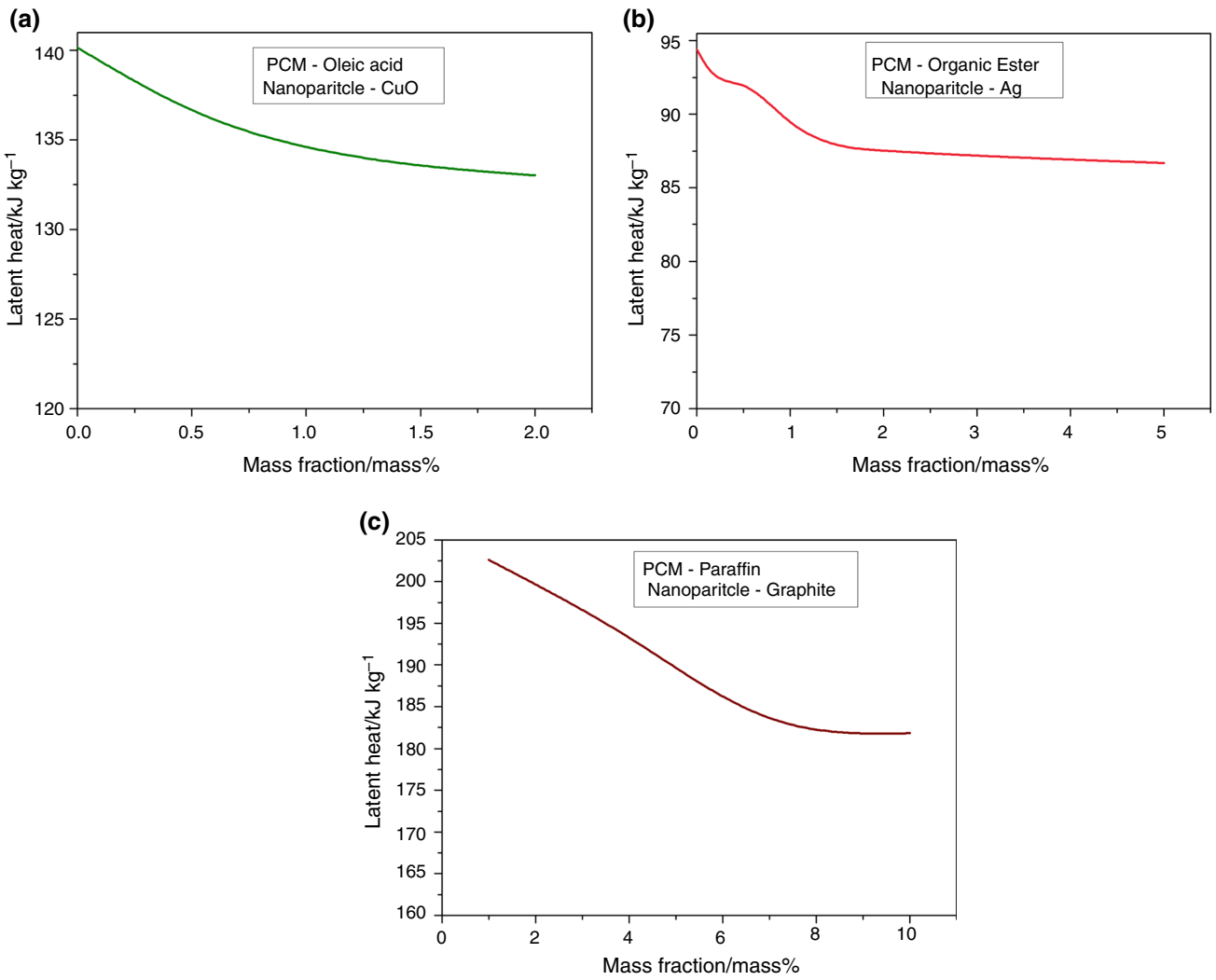

Fig. 6 Variation of latent heat with particle loading: **a** CuO [36], **b** Ag [34], **c** graphite [47]

Table 4 Salient features of nanofluids interfacial mechanisms

Mechanism	Features
Brownian motion	Microscopic random motion of particles
	Increases as the particle size reduces
	Leads to collision between particles
	Enhancing thermal conductivity in two ways:
	1. Particle diffusion
	2. Microconvection of liquid around particles
	Reducing latent heat by weakening fluid molecular bond
Interfacial liquid layering	Liquid layering at the interface of the particles
	Due to van der Waals forces
	Atomic structure of the layer is more ordered than that of bulk liquid
	Results in more effective volume and contributes to the increase in effective thermal conductivity
	Molecular bonds between layered liquids get weakened, and thus reduction in latent heat
Particles clustering	Particles form percolating structures due to intra molecular forces
	Effective volume of clustered molecules is greater than physical volume
	Forming high-conductivity network which leads to higher effective thermal conductivity
	Results in higher viscosity

the latent heat of PCM as smaller particles exhibit strong intramolecular attraction with base fluid molecules. Since none of the nanomaterials employed in the work was tested with a range of diameters, it cannot be concluded that the latent heat gets increased as the size of the particles decreases. On the other hand, Zabalegui et al. [68] have proved that smaller particles affect significant reduction in latent heat.

The reduction in the latent heat is generally due the volume occupied by the nanoparticles which does not undergo phase change. However, Zabalegui et al. [84] have pointed that some more volume also does not contribute to the phase change as this additional volume possesses weak molecular bond structure. It is obvious that the energy required to break down the weak molecular bond would be less during melting. According to the authors, the strained volume could be a consequence of three interfacial mechanisms including Brownian motion and it is further stated that all the three mechanisms are highly pronounced when the particle size is small. Since the details of the three mechanisms are beyond the scope of this review, the essence of the same is presented in Table 4.

Viscosity of composites

As stated already, heat transfer during melting of PCM is primarily governed by natural convection in the liquid PCM. This is because of the stronger buoyancy-driven flows existing in the molten PCM. The existence of buoyancy-driven flows is found in various types of configurations of LHTESS modules by earlier works [92–94]. If the presence of nanoadditives in the PCM by any means hampers the buoyancy-driven flows, then it would result in lesser convective coefficient. Hence, the net heat transfer rate may not be on higher side despite considerable enhancement in thermal conductivity. Since buoyancy-driven natural convection is determined by viscous force, viscosity of the PCM is critical parameter to be analysed. Moreover, it is important to understand how significantly nanoadditives affect the viscosity of PCM.

Kole and Dey [95] have emphasized that viscosity of nanofluids employed for heat transfer applications should be treated as significant as thermal conductivity. However, Mahbubul et al. [96] have expressed in their recent review that research on nanofluids primarily revolves around thermal conductivity only. Although the statement is derived from works on general heat transfer, it is also applicable in case of works concerning PCMs.

He et al. [39] have demonstrated that the viscosity of water increases with increase in volume fraction of TiO_2 nanoparticles. Though the increase is nonlinear, it is quite significant. As the concentration increases, the particles come closer, and hence, the frictional force between the particles and base fluid molecules increases. The results of Jesumathy et al. [37] are in agreement with those of He et al. [39] as viscosity of paraffin wax shows increasing tendency with mass fraction of CuO. Although Arasu et al. [60] have reported similar findings for Al_2O_3 and CuO in paraffin wax, it is found that the increase in dynamic viscosity is more pronounced with CuO than with Al_2O_3. Further, the viscosity of PCM with any concentration of both the nanoadditives is inversely proportional to

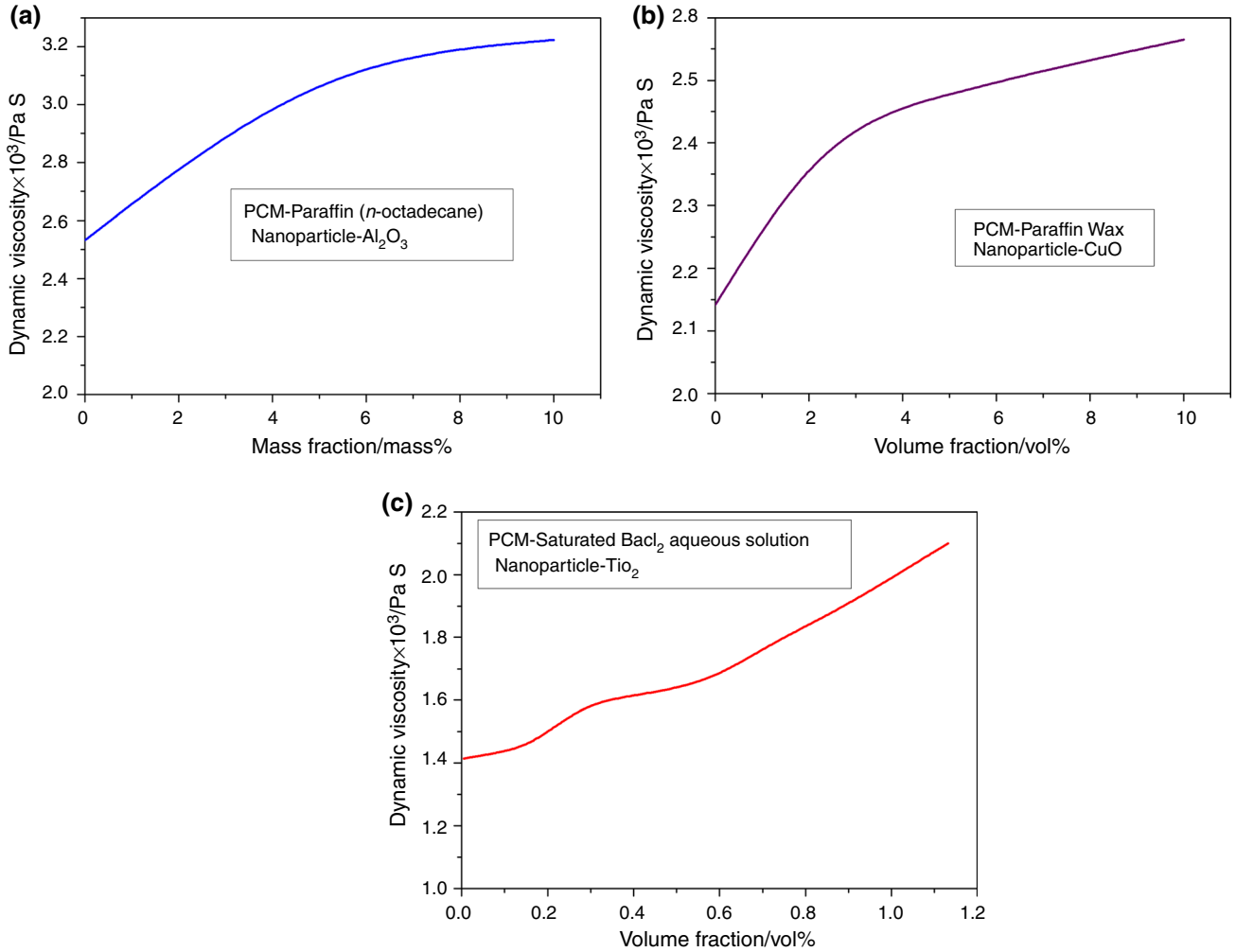

Fig. 7 Variation of viscosity with particle loading: **a** Al_2O_3 [38], **b** CuO [37], **c** TiO_2 [39]

temperature. At the same time, Mostafavinia et al. [97] have revealed that the effect of particle fraction on viscosity is more appreciable at relatively low temperature.

According to Ho and Gao [38], nanoadditives show much stronger influence on viscosity in comparison with the influence on thermal conductivity (four to ten times more). The increase in viscosity of nanofluids as additive loading increases is consistently reported by many researchers [96]. The same can be verified from Fig. 7. Nevertheless, roles of shape/size of the additives in altering the viscosity of PCMs are yet to be explored as none of the above-mentioned works has analysed the same. Even it is proved that more amounts of additives brings in benefit in terms of higher thermal conductivity, the amount should be limited from viscosity perspective. The clear understanding of relation between size/shape and viscosity would be more helpful in choosing optimum fraction of additives. This demands a lot more work in future.

In addition to viscosity evaluation, it is crucial to get the insights of rheological behaviour to understand the convective heat transfer in nanofluids [98]. Sridhara and Satapathy [99] have indicated the possibility of non-Newtonian behaviour of nanofluids in their review article. In case of nano-PCM research, Kumaresan et al. [52] have studied the Newtonian behaviour of MWCNT-dispersed paraffin wax. It is found that only in low shear stress range (0–1 Pa), the viscosity of composites decreases with increase in shear stress. Thereafter, the increase in shear stress could not make any change in viscosity. It seems that the nano-PCM composites show shear thinning behaviour at low shear stress range and behave as Newtonian fluids thereafter. The shear thinning behaviour is found more severe when the fraction of nanoadditives is higher. Nevertheless, all tested composites are observed with considerable shear thinning behaviour at low shear stress range. Similarly, Motahar et al. [100] have stated that the non-Newtonian behaviour of nonofluids does not depend only on shear rate but also on particle concentration and viscosity of base fluid. It is proved by the same authors [64] in the other work in which the non-Newtonian behaviour of *n*-

octadecane added with mesoporous silica particles is observed when the mass fraction of particles is greater than 3%. However, Pak and Cho [101] have found that the shear thinning behaviour of nanofluids begins only after some amount of nanoadditives loading and the volume fraction at which shear thinning behaviour begins varies depending upon the type of nanoadditives. Over and above, the non-Newtonian behaviour itself is questionable as some researchers claim that the nanofluids are generally Newtonian [83, 102].

In spite of having good number of publications on rheology of single-phase nanofluids, there is no firm conclusion yet on the same. As far as PCM-based nanofluids are concerned, only few studies could be found to understand the rheology. Hence, the future studies should have more focus on addressing the rheological issues.

Heat transfer enhancement

As far as PCMs are concerned, the heat transfer enhancement is generally gauged in terms of reduction in melting or solidification time after adding nanomaterials. As the nanoadditives are used as thermal conductivity enhancers, the melting or solidification rate of PCM is expected to be higher which means that the nanoadditives would lead to significant reduction in melting/solidification time. However, nanoparticles in the PCM not only alter the thermal conductivity but also other properties like viscosity and latent heat which is already elaborated. Moreover, the distribution of particles in the PCM may not be uniform and is indifferent in solid and liquid PCMs. One can suspect that these things affect the phase change process. Hence, it is also important to look into enhancement in melting/solidification rate rather making judgment based on only thermal conductivity enhancement.

Melting rate enhancement

The influence of Cu nanoparticles on the melting process of Erythritol stored in concentric cylinder configuration is studied by Abolghasemi et al. [24]. It is shown that the time required for complete melting could be substantially reduced by nano-Cu and the decrease in melting time seems to be monotonous with particle loading. However, a firm conclusion cannot be drawn from these findings as the results are contradictory to that of Arasu and Mujumdar [103] and Arasu et al. [59].

Arasu and Mujumdar [103] have observed that the melting rate of PCM in a square enclosure increases slightly only if small amount of AlO_2 is added (2 mass%). Beyond the said quantity, addition of particles tends to decrease the melting rate. Similarly, Arasu et al. [59] have shown that the enhancement in phase change rate of PCM in a concentric double pipe module is significant only during solidification, and thus, it is recommended to use lower fraction of nanoadditives for better cyclic performance.

Although all the above three works are based on numerical modelling, the discrepancy between the results of the former and those of other two is due to the inclusion of natural convection in the modelling. The numerical modelling by Abolghasemi et al. [24] has not taken into account the natural convection which means that the role of increased viscosity is ignored. For the applications wherein single-phase fluids are involved, the thermal conductivity improvement is given greater importance as it accelerates the conduction heat transfer. It is known that increase in viscosity due to the presence of nanoadditives suppresses the convection heat transfer. Since such applications mostly encounter forced convection, the diminished rate of convection heat transfer due to higher viscosity can be balanced by increased velocity of the flowing fluid. Hence, the overall heat transfer enhancement is expected to be in line with the enhancement in thermal conductivity. On the other hand, the case of PCMs looks different as the overall heat transfer rate may not be necessarily higher in the same order of thermal conductivity increase. It is clear that nanoadditives tend to suppress the natural convection during melting which can be validated by the findings of Ho and Gao [104]. Ho and Gao [104] conducted experiments on the melting of alumina nanoparticles-dispersed *n*-octadecane in a vertical enclosure. The heat transfer performance is reported in terms of surface-averaged Nusselt number at the hot wall. Although the surface-averaged Nusselt number is high in the beginning, the same becomes lesser as the natural convection dominates the heat transfer. This indicates the dampened natural convection which of course is due to particle addition.

Hence, the extent to which heat transfer rate can be augmented due to increase in thermal conductivity despite the handicapped thermal convection is to be quantified. Significant number of works is reported on the relation between particle loading and melting rate. Sciacovelli et al. [105] added copper nanoparticles to enhance the melting rate of paraffin wax in the LHTESS which is a shell and tube module. The computational modelling takes into account the convection in liquid PCM using the effective viscosity evaluated in terms of particle concentration. The enhancement in heat transfer rate is evaluated in terms of reduction in melting time and rise in liquid fraction. The maximum reduction in melting time with 4% volume fraction is reported as 15%. Similar numerical model was adopted by Hosseini et al. [106] to investigate the melting of copper particles added paraffin wax (RT50). Although both Sciacovelli et al. [105] and Hosseini et al. [106] have used shell and tube module, the former considered the vertically oriented system whereas the latter used

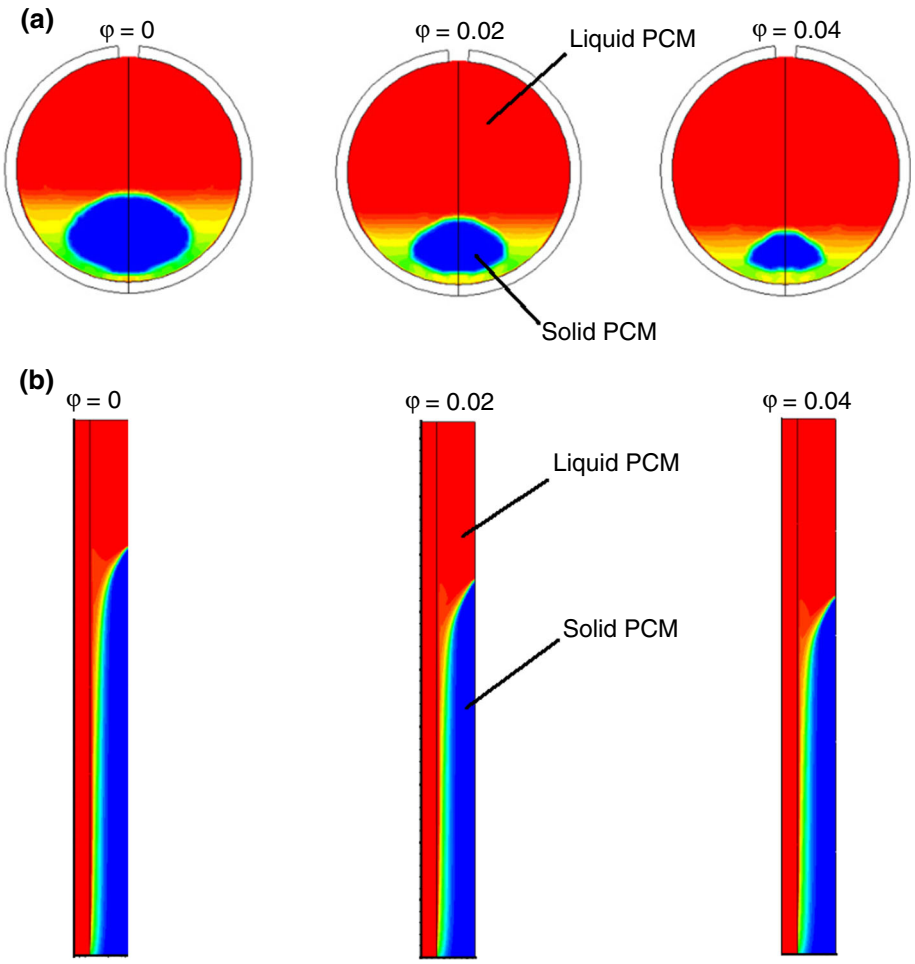

Fig. 8 Melting rate enhancement due to nanoadditives: **a** melting status in a spherical container after 8 min [21], **b** melting status in a vertical shell and tube arrangement after 4000 s [105]

horizontal one. Hosseini et al. [106] have reported heat transfer enhancement even up to 5% volume fraction of particles (maximum of 14.6%). It is also highlighted that the reduction in melting time and increase in liquid fraction are the result of increased penetration velocity of melt front. Although no attempt is made by both the works to determine the optimum volume fraction, it can be interpreted from the results that the enhancement in heat transfer with increase in particle addition is nonlinear.

Jourabian et al. [107] have investigated the melting of Cu particles added water (PCM) in an annulus. Although the melting rate enhancement is observed at all volume fraction of particles (0.01% and 0.02%), the enhancement effect is less pronounced at 0.02% as compared to 0.01%. Through series of numerical and experimental works, Dhaidan et al. [108–110] have observed that the enhancement in melting rate becomes less at higher particle fractions when the CuO added *n*-octadecane was melted whether in square container or in annular container or in cylindrical capsule. The nonlinear increase in melting rate of paraffin wax with Cu particles loading is also experimentally proved by Wu et al. [111]. The authors have revealed that the melting time could be reduced by 27% when 0.5% mass of Cu particles were added, but the reduction was only 32% when loading was doubled. Similarly, Patil and Dey [112] could achieve reduction of 6.52%, 10.86% and 13.0%, respectively, with CuO mass% of 0.33, 0.66 and 1 for paraffin wax. In case of alumina, 1 mass% resulted in 20% reduction, whereas it was only 29% even the mass% was increased to 5 [113].

Considering the preceding discussion, it can be stated that the melting rate of PCM cannot be monotonously increased by increasing the concentration of nanoadditives. However, the findings of Harikrishnan and Kalaiselvem [63] show that the monotonous heat transfer enhancement is possible only up to a small fraction of particle loading. The authors could achieve reduction in melting time of 6.43%, 14.62% and 21.05%, respectively, with 0.1, 0.2 and 0.3 mass% of TiO_2. Similar observations are made by Hajare and Gawali [114] who used TiO_2 and Al_2O_3 with maximum fraction of 0.075%.

Whether the melting rate enhancement is linear or nonlinear with nanomaterials loading, it would be appreciable as long as significant enhancement is achieved

through nanomaterials. Figure 8 exhibits the enhancement in melting rate due to addition of nanomaterials. However, the enhanced viscosity due to nanomaterials might become dominant over enhanced thermal conductivity at some point of time which would result in adverse effect on melting rate. This necessitates the determination of the optimum fraction of nanoparticles beyond which reduction in convection heat transfer overcomes the enhancement in conduction heat transfer. This would be helpful in achieving enhanced overall melting rate.

While investigating the impact of locations of two pairs of source–sink (positioned on sidewalls of a square container) on the melting performance of Al_2O_3 added paraffin wax, Ebrahimi and Dadvand [115] attempted to determine the optimum volume fraction of nanoadditives. Based on the locations of source–sink pairs, four cases were considered and among the two particle fractions considered (volume fractions 2% and 5%), 2% exhibited highest melting rate in all cases. Further, PCM with 5% volume fraction is proven to be inferior to pure PCM in terms of melting rate in two of the four cases considered. Mostafavinia et al. [97] have also carried out similar work with similar module, PCM and nanoparticles except the one with respect the location of the source–sink. These results also confirm the optimum fraction as 2%. On the other hand, Auriemma and Lazzetta [116] have shown that even volume fraction of 3% results in lower melting rate as compared to pure PCM. The numerical work focuses on melting of paraffin wax added with three different nanomaterials (Al_2O_3, CuO, ZnO) in a rectangular container. Among the three composites, CuO- and ZnO-added samples are observed with lower melting rate when the volume fraction is 3% than the pure PCM. Although 3% volume fraction Al_2O_3 has not reduced the melting rate, the difference in melting rate between pure PCM and PCM with Al_2O_3 of 3% volume fraction is insignificant. By looking at the similarity between the modules considered in the above works, 2% volume fraction may be considered as optimum volume fraction for highest melting rate. Murugan et al. [117] have predicted even lower value, i.e. 0.3% mass fraction as optimum value of MWCNT for paraffin wax.

However, higher fractions are also found as optimum values by few authors. Naeem et al. [26] have investigated the melting performance of Cu nanoparticle- and TiO_2 nanoparticle-dispersed paraffin wax. The melting process of PCM in spherical capsules was analysed with mass fractions of 1%, 2%, 3% and 5%, and highest enhancement is observed with 3 mass%. Lokesh et al. [118] have also observed 3 mass% as optimum fraction since MWCNT of 3 mass% could achieve highest reduction in melting time of paraffin wax in cylindrical capsule. Bashar [119] has reported even higher value as optimum fraction of CuO, i.e. 6% mass fraction. According to the findings, paraffin wax with this concentration has established highest melting rate throughout the charging process in a rectangular container. As a novel way of employing nanoadditives, Esfe et al. [120] investigated the thermal conductivity enhancement of ethylene glycol through hybrid nanoadditives (70% alumina and 30% SWCNT). In this case, the enhancement could be achieved up to a volume fraction of 2.5% whereas with single additive (SWCNT), the optimum fraction was only 1%.

The limited works reported on the optimum fraction of nanoparticles in PCM have recommended both lower and higher quantities as optimum quantity. The discrepancy between the findings of various works is due to the assorted influencing levels of natural convection in different cases during melting. It can be understood that the buoyancy force induced natural convection is dependent on thermophysical properties of PCM and dimensions/configuration of the storage module [121]. Moreover, the orientation of the heat source has critical effect on the strength of natural convection. In fact, Sun et al. [122, 123] have observed that the natural convection is highly influential on melting rate when the PCM is heated from the side as compared to the case where the heat source is at the bottom. It is clear from the above that the melting process of pure PCM cannot be accelerated by natural convection in similar fashion in all cases. As a matter of fact, the natural convection is less pronounced in some cases. Hence, the quantity of nanoparticles added into the PCM should be kept lower if the natural convection is highly influential and vice versa. Overall, the optimum quantity should be decided based on the combination of PCM/nanomaterial, geometry/size of the container and orientation of the heat source. It should also be considered that the higher particles concentration may affect the stability of nano-PCM due to agglomeration. The summary of the reported works focusing on melting rate enhancement due to nanoadditives is given in Table 5.

Solidification rate enhancement

As it is known that the solidification of PCM is governed by conduction heat transfer, the high thermal conductivity of particles is expected to play more dominating role in affecting the solidification rate. According to Chandrasekaran et al. [124], even 0.1 mass% of CuO in deionized (DI) water could reduce the solidification time by 35%. The experimental work on solidification of this nano-PCM in spherical capsule is not extended to explore effect of varying concentration of nanoparticles on solidification rate.

Sebti et al. [125] have observed reduction in solidification time of 8% and 16%, respectively, with 2.5% and 5% volume fraction of Cu particles in water when the numerical test was carried out with horizontal concentric annulus.

Table 5 Summary of reports on enhancement of melting rate

References	PCM	Nanomaterial	Maximum fraction	Optimum fraction	Phase change process	Maximum enhancement
Hajare and Gawali [114]	Paraffin wax	Al_2O_3 and TiO_2	0.075 mass%	–	Melting	5.92% for 0.05 mass% TiO_2
Patil and Dey [112]	Paraffin wax	Al_2O_3 and CuO	1 mass%	–	Melting	Melting time reduced by 20 min for Al_2O_3 and by 15.6 min for CuO
Pise et al. [113]	Paraffin wax	Al_2O_3	5 mass%	–	Melting	Melting time reduced by 29%
Harikrishnan and Kalaiselvam [63]	Palmitic acid	TiO_2	0.3 mass%	–	Melting	Melting time reduced by 21.05%
Sciacovelli et al. [105]	Paraffin wax	Cu	5 vol%	–	Melting	Melting time reduced by 15%
Wu et al. [111]	Paraffin wax	Cu	1 mass%	–	Melting	Melting time reduced by 33%
Hosseini et al. [106]	Paraffin wax	Cu	5 vol%	–	Melting	Melting time reduced by 14.6%
Hosseinizadeh et al. [21]	Paraffin wax	Cu	5 vol%	–	Melting	Melting time reduced by 27.7%
Ebrahimi and Dadvand [115]	Paraffin wax	Al_2O_3	5 vol%	2 vol%	Melting	Time for 50% melting is reduced by 9%
Auriemma and Iazzetta [116]	Paraffin wax	Al_2O_3, TiO_2 and CuO	3 vol%	1 vol%	Melting	Melting rate is lower for 3 vol% compared to pure PCM
Lokesh et al. [118]	Paraffin wax	MWCNT	0.9 mass%	0.9 mass%	Melting	Melting time reduced by 29%
Naeem et al. [26]	Paraffin wax	Cu and TiO_2	5 mass%	3 mass%	Melting	Melting time reduced by 33% for Cu
Murugan et al. [117]	Paraffin wax	MWCNT	0.9 mass%	0.3 mass%	Melting	Melting time reduced by 30%

Kashani et al. [126] have also taken same combination of PCM and nanoparticles to numerically investigate the solidification in vertical enclosure. The authors could observe 15% reduction in solidification time with 5% volume fraction of Cu particles, whereas the reduction was about 32% when the volume fraction was 10%. Using the similar module, the solidification of paraffin wax under the influence of Cu particles was studied by Mahato et al. [127]. The time for complete solidification could be reduced by 9% with 2.5% volume fraction and by 18% when volume fraction was increased to 5%. Mehdi and Nsofor [128] have also found 8% reduction in solidification time by adding 3% of alumina particles in paraffin wax.

Hosseini et al. [129] too have used vertical enclosure for the numerical investigation of solidification of water dispersed with three different nanoparticles, i.e. Cu, TiO_2 and Al_2O_3. Although the results are not presented in the form of solidification rate/solidification time, the results of Nusselt number would prompt one to observe similar trends as that of Kashani et al. [126] even up to 20% volume fraction.

It is evident from the above findings that the solidification rate of PCM can be enhanced more or less linearly with increase in quantity of nanoparticles. This can be verified from the results of the earlier works which are compiled in Fig. 9. Besides these numerical studies, results of few experimental investigations which highlight the linear dependency of solidification rate on particle fraction seem to be noteworthy. Sathishkumar et al. [130] analysed the solidification rate of grapheme nanoplatelets-added DI water in spherical capsule. The authors have used nanoplatelets of 0.2%, 0.4% and 0.6% mass fraction and have confirmed the linear enhancement in solidification rate. The experimental work of Suresh Kumar and Kalaiselvam [131] has also shown linear enhancement in the solidification rate of palmitic acid which was added with CuO of 0.3 to 0.8% mass fraction in spherical/cylindrical capsules. Temirel [132] conducted experiments on the solidification of eicosane in spherical shell. Although the author has considered relatively higher concentrations of xGnP (1.5, 3 and 4.5%) as compared to Sathishkumar et al. [130], the enhancement rate exhibits similar trend.

On the other hand, the nonlinear enhancement in solidification rate can also be found in the results of few investigations. One such work is by Sharma and Ganesan [133] which is a part of other work by Sharma [134] in which water is the PCM and Cu nanoparticles are used for

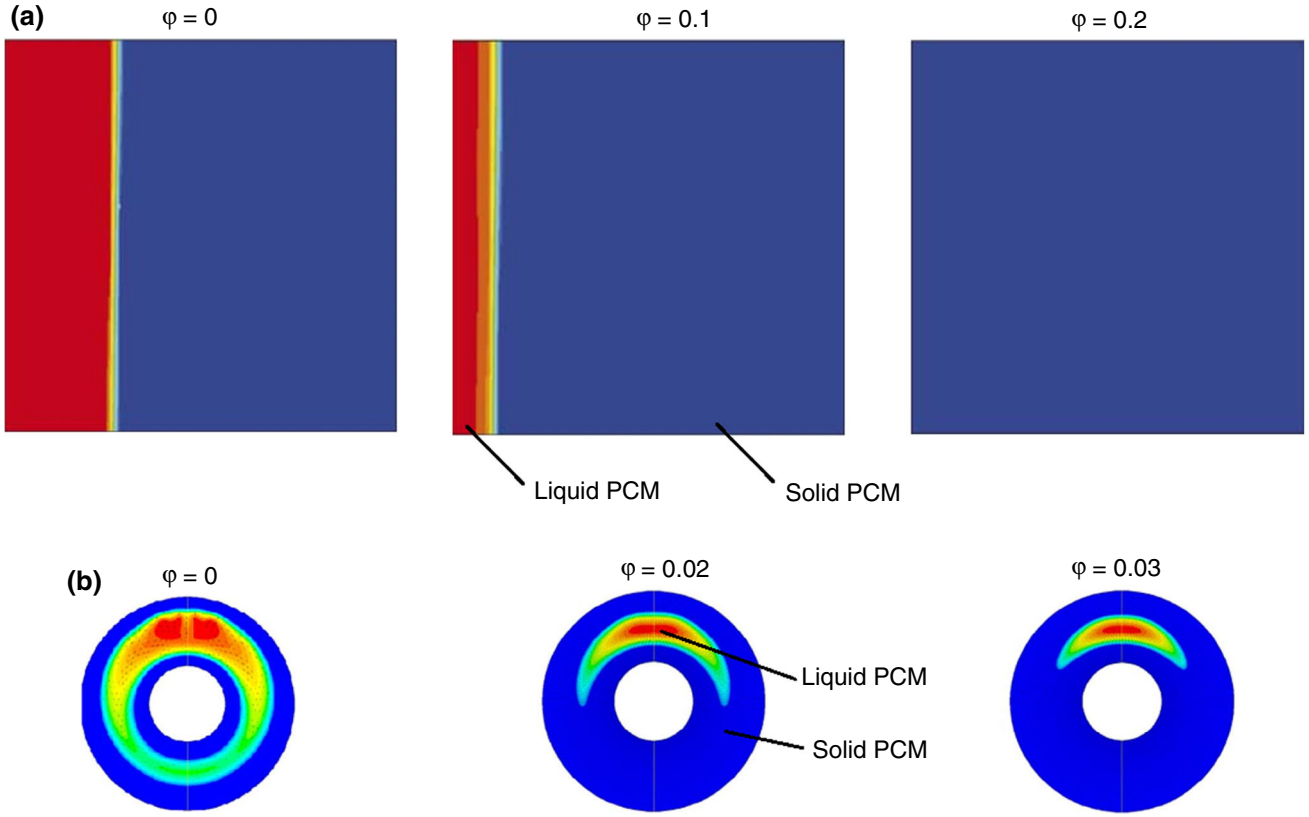

Fig. 9 Solidification rate enhancement due to nanoadditives: **a** solidification status in a square cavity after 1500 S [30], **b** solidification status in annular space after 5 h [128]

reducing the solidification time in trapezoidal cavity. As reported, the solidification time could be saved by 40% and 53%, respectively, with particle volume fraction of 10% and 20%. The nonlinear relation between solidification rate and particle fraction is also exposed experimentally by Fan and Khodadadi [61]. The authors prepared Cu particles added cyclohexane and have found non-monotonic enhancement of solidification rate once the mass fraction is more than 2%. This is because of nonlinear enhancement of solid phase thermal conductivity although the thermal conductivity of liquid phase exhibits monotonic enhancement with particle fraction.

Unlike melting, the dampening effect on natural convection due to nanoadditives does not pose any serious problem when it comes to solidification rate. This may prompt to use higher fraction of particles if solidification rate is prioritized. For example, in solar thermal applications, solar energy is stored during long day time whereas the retrieval of energy is to be done in the short late evening hours/night hours. This requires higher solidification rate of the PCM even if the melting rate is slower.

The linear enhancement of solidification rate is not always possible especially with higher fractions; for example, above mass fraction of 2% or volume fraction of 10%, the solidification rate may not be significant even though the same may keep increasing. Hence, it is better to use smaller quantity of nanoparticles from the perspective of achieving cost saving, higher energy storage density, stable nano-PCM and higher number of thermal cycles.

Apart from particle fraction, particle size has significant effect on solidification rate according to El Hasadi and Khodadadi [135]. The solidification of water dispersed with Cu particles of diameter 5 nm and 2 nm in a square cavity is analysed. The numerical results show that decreasing particle size leads to slower solidification as smaller particles tend to lower the solidus temperature as a result of constitutional supercooling. The earlier works concerning enhancement of solidification rate due to nanoadditives are listed in Table 6.

Prediction of thermo-physical properties

As discussed in "Nanomaterials and thermo-physical properties of composites" section, the change in thermo-physical properties of PCMs due to nanoadditives determines the thermal performance improvement. Hence, characterization of nanomaterials added PCM remains as

Table 6 Summary of reports on enhancement of solidification rate

Reference	PCM	Nanomaterial	Maximum fraction	Optimum fraction	Phase change process	Maximum enhancement
Harikrishnan and Kalaiselvam [36]	Oleic acid	CuO	0.6 mass%	–	Solidification	Solidification time reduced by 27.6%
Chandrasekaran et al. [124]	Deionized (DI) water	CuO	0.1 mass%	–	Solidification	Solidification time reduced by 35%
Sebti et al. [125]	Water (base fluid)	Cu	0.05 vol%	–	Solidification	Solidification time reduced by 16%
Kashani et al. [126]	Water (base fluid)	Cu	10 vol%	–	Solidification	Solidification time reduced by 32%
Mahato et al. [127]	Paraffin wax	Cu	5 vol%		Solidification	Solidification time reduced by 18%
Hosseini et al. [129]	Water (base fluid)	CuO, Al_2O_3, TiO_2	20 vol%	–	Solidification	Solidification time reduced by 16%
Sathishkumar et al. [130]	Deionized (DI) water	GNP	0.6 mass%	–	Solidification	Solidification time reduced by 24%
Temirel [132]	Eicosane	xGNPs	4.5 mass%	–	Solidification	Solidification time reduced by 51% for small sphere and by 53% for large sphere
Sharma and Ganesan [133]	Water (base fluid)	Cu	20 vol%	–	Solidification	Solidification time reduced by 57%
Sharma [134]	Water (base fluid)	Cu	20 vol%	–	Solidification	Solidification time reduced by 53%
Fan and Khodadadi [61]	Cyclohexane	CuO	4 mass%	2 mass%	Solidification	Solidification time reduced by 5.2% for 2 mass% of CuO experimentally and by 8.09% in numerical prediction
El Hasadi and Khodadadi [135]	Water	CuO	10 mass%	–	Solidification	Solidification rate decreases with particle size

one of the critical activities of the concerned research. Although highly advanced instrumentation and well-established measurement techniques are available, testing nano-PCM for various quantities of nanoadditives is time-consuming and is highly expensive. On the other hand, employing theoretical/empirical relations results in reasonable prediction quickly but with zero cost. Moreover, the relations are more useful when it comes to numerical modelling-based research.

The thermo-physical properties of the nanofluid are a combination of the properties of the nanoadditive and the base fluid, and hence, the additive causes significant change in the properties of resultant fluid depending on the concentration. Hence, the relations for the properties of mixture should be expressed as a function of mass/volume fraction of additives in the mixture. However, the nanomaterial size, shape and more importantly the particle dynamics are also to be taken into account wherever applicable. In this perspective, researchers have developed various models for predicting the properties of nanofluids. This section reviews the models developed so far and their applicability for nano-PCMs.

Density and specific heat models

To be specific, density of the fluid plays a very important role wherever natural convection is involved like in the case of PCMs. Since buoyancy force is directly related to natural convection and is determined by density gradient, the magnitude of natural convection is influenced by density.

To determine density, a simple and straightforward model known as "Classical Mixture Model" is employed in most of the works concerning PCMs [20, 25, 136–138]. Here, the density of nanofluid (ρ_{nf}) is evaluated as follows.

$$\rho_{nf} = \varphi\rho_p + (1-\varphi)\rho_f \quad (1)$$

where φ is the volume fraction of the nanomaterial, ρ_p and ρ_f are the density of the nanomaterial and the base fluid (PCM), respectively.

Equation (1) considers a linear relation between density of the mixture and the concentration of the nanoadditive. Further, it is expressed as a function of only the additive's concentration.

However, Sharifpur et al. [139] claims that the mixture model over predicts the density and the deviation widens up as the volume fraction increases. The authors have further suggested taking into account the nanolayer in order to overcome the deviations. The nanolayer is nothing but the interfacial layer exists in the solid–liquid interface. The nanolayer is thus assumed as a void, and the void thickness is expressed in terms of particle size. The resulting equation would be an empirical relation. The inclusion of void thickness results in lesser volume fraction of particles than the usually calculated one. The effective volume fraction is given by

$$\varphi_{\text{eff}} = \frac{1}{\frac{1}{\varphi} - 1 + \left(r_{\text{p}} + t_{\text{v}}\right)^3 / r_{\text{p}}^3} \tag{2}$$

Following Eq. (2), the modified equation for the density of nanofluid is written as

$$\rho_{\text{nf(modified)}} = \frac{\rho_{\text{nf}}}{(1-\varphi) + \varphi\left(r_{\text{p}} + t_{\text{v}}\right)^3 / r_{\text{p}}^3} \tag{3}$$

where r_{p} is the radius of the particles and t_{v} is the thickness of the nanolayer.

Equation (3) includes the effects of size and thickness of the particles besides the volume fraction. Although the model is proved to be more accurate and simple, the calculation is not as straightforward as with the case of mixture model. This is because the calculation of thickness needs experimental data. The model makes good prediction even up to a volume fraction of 1%.

The specific heat also plays a key influencing role when it comes to heat transfer performance. By adding nanoparticles in the heat transfer fluid, the ability to conduct the heat is enhanced. This would result in lower specific heat in comparison with the base fluid. Similar to density, specific heat of nanofluids (c_{nf}) is calculated using the law of mixture [140–142].

$$c_{\text{nf}} = \frac{(1-\varphi)\rho_{\text{f}} c_{\text{f}} + \varphi\rho_{\text{p}} c_{\text{p}}}{(1-\varphi)\rho_{\text{f}} + \varphi\rho_{\text{p}}} \tag{4}$$

where c_{p} and c_{f} are the specific heat of the nanoadditives and the base fluid, respectively.

The density and specific heat can simultaneously be determined by combining Eqs. (1) and (4) [143].

$$\rho_{\text{nf}} c_{\text{nf}} = \varphi\rho_{\text{p}} c_{\text{p}} + (1-\varphi)\rho_{\text{f}} c_{\text{f}} \tag{5}$$

According to Wang et al. [144], the specific heat of nanofluid increases as the particle size decreases. The increased surface energy due to decreased size results in higher specific heat. Hence, one may demand expressing specific heat in terms of particle size along with volume fraction. However, further works [145, 146] have revealed that effect of particle size on specific heat of nanofluids is negligible.

Thermal conductivity models

Unlike density and specific heat, evaluation of effective thermal conductivity of nanofluids is bit challenging. Although plenty of models are developed for effective thermal conductivity, until now, reliable and complete solution is yet to be achieved.

In the simple approach, the effective thermal conductivity of nanofluids (k_{nf}) is predicted using the well-known Maxwell equation [147],

$$k_{\text{nf}} = k_{\text{f}}\left[\frac{k_{\text{p}} + 2k_{\text{f}} + 2\varphi\left(k_{\text{p}} - k_{\text{f}}\right)}{k_{\text{p}} + 2k_{\text{f}} - \varphi\left(k_{\text{p}} - k_{\text{f}}\right)}\right] \tag{6}$$

where k_{p} and k_{f} are the thermal conductivity of the nanoadditives and the base fluid, respectively.

However, Eq. (6) holds good for the cases when larger (micro), spherical particles are added in small concentrations. Following Maxwell, Bruggeman [148] came out with a model which is again for the micron sized particles.

$$\varphi\left(\frac{k_{\text{p}} - k_{\text{nf}}}{k_{\text{p}} + 2k_{\text{nf}}}\right) + (1-\varphi)\left(\frac{k_{\text{f}} - k_{\text{nf}}}{k_{\text{f}} + 2k_{\text{nf}}}\right) = 0 \tag{7}$$

Unlike Maxwell's one, Bruggeman's model is found to be satisfactory even for higher concentrations [149]. In the later year, another model applicable to even non-spherical particles was proposed by Hamilton and Crosser [150]. The shape of the particles is accounted for by including a shape function (n).

$$k_{\text{nf}} = k_{\text{f}}\left[\frac{k_{\text{p}} + (n-1)k_{\text{f}} - (n-1)\varphi\left(k_{\text{f}} - k_{\text{p}}\right)}{k_{\text{p}} + (n-1)k_{\text{f}} + \varphi\left(k_{\text{f}} - k_{\text{p}}\right)}\right] \tag{8}$$

Here, the shape function is given as $n = 3/\psi$, where ψ is the sphericity.

$$\text{Sphericity} = \frac{\text{Surface area of the sphere whose volume is equal that of the particles of actual size}}{\text{Surface area of the particles of actual size}}$$

Accordingly, researchers considered value for sphericity ranging from 0.3 to 1 [143].

Looking at the deliberated three models, it is understood that only the concentration and shape of the nanoadditives are taken into account. Hence, these models have measured the heat transfer mechanism at macroscopic level only (i.e. diffusive heat transfer in base fluid and particles).

As stated in "Latent heat of composites" section, the enhancement in heat transfer of nanofluids is governed by interfacial mechanisms and the models discussed above have not considered the effects of these mechanisms. In view of this, researchers have proposed quiet a number of models with inclusion of effects of heat transfer enhancement mechanisms.

Models with effects of interfacial layers

According to Yu and Choi [151], the thermal conductivity of nanoadditives is to be altered in order to take into account the effects of nanolayer. Accordingly, the thermal conductivity ($k_{p,m}$) is expressed as

$$k_{p,m} = k_p \left[\frac{2(1-\gamma) + (1+\beta)^3(1+2\gamma)\gamma}{-(1-\gamma) + (1+\beta)^3(1+2\gamma)} \right] \tag{9}$$

where γ is the ratio of the thermal conductivity of nanolayer to that of nanoadditives and β is the ratio of the thickness of the nanolayer to the radius of the particle.

Now, the expression for effective thermal conductivity is rewritten using Maxwell's model

$$k_{nf} = k_f \left[\frac{k_{p,m} + 2k_f + 2\varphi(k_{p,m} - k_f)(1+\beta)^3}{k_{p,m} + 2k_f - \varphi(k_{p,m} - k_f)(1+\beta)^3} \right] \tag{10}$$

As the above model is applicable to only spherical particles, the same authors [152] modified the Hamilton–Crosser model by including the effect of nanolayer in order to make it applicable to non-spherical particles.

$$k_{nf} = \left\{ 1 + \frac{\left[\frac{1}{3}\sum_{j=a,b,c}\left(k_{pj} - k_f\right)/k_{pj} + (n-1)k_f\right] n\varphi_{eff}}{1 - \left[\frac{1}{3}\sum_{j=a,b,c}\left(k_{pj} - k_f\right)/k_{pj} + (n-1)k_f\right]\varphi_{eff}} \right\} k_f \tag{11}$$

Besides the above models, the literature presents few more thermal conductivity models which consider the effects of nanolayer [153–155]. The summary of these models along with their features can be found in Table 7.

Models with effects of Brownian motion

As the heat transfer enhancement due to Brownian motion involves random motions of particles, the effective thermal conductivity should take into account the diameter of the particles/surface geometry (nanostructure) and the particles' dynamics [156]. The representative models which include the Brownian motion effects [157–160] are presented in Table 8.

In nano-PCM works, almost all have adopted either the Koo and Kleinstreuer [161] model or the one proposed by Amiri and Vafai [162]. In Koo and Kleinstreuer [161] model, the effective thermal conductivity is evaluated by adding the increase in thermal conductivity as a result of Brownian motion to the thermal conductivity estimated using Maxwell's model. The first part is found to be a function of particles' size/concentration, temperature and other properties of both particles and base fluid. Accordingly, the resultant equation is given as,

$$k_{nf} = k_f \left[\frac{k_p + 2k_f + 2\varphi(k_p - k_f)}{k_p + 2k_f - \varphi(k_p - k_f)} \right] + 5 \times 10^4 \alpha\varphi\rho_f c_f f(T,\varphi) \sqrt{\frac{K_B T}{\rho_f 2r_p}} \tag{12}$$

where $K_B = 1.381 \times 10^{-23}$ J K^{-1} is the Boltzmann constant and α is the volume fraction of base fluid moving with a particle caused by Brownian motion. The function $f(T, \varphi)$ in Eq. (12) includes the enhanced temperature (T) dependence. Evaluation of α and f needs extensive experimental data. For nano-PCM composites, the empirical relations given in Eqs. (13) and (14) are generally employed by researchers [25, 60, 163].

$$\alpha = X(100\varphi)^Y \tag{13}$$

$$f(T,\varphi) = (A\varphi + B)\frac{T}{T_{ref}} + (C\varphi + D) \tag{14}$$

where X, Y, A, B, C and D are the experimentally obtained constants and T_{ref} is the reference temperature = 273 K.

Besides the above model, the model proposed by Amiri and Vafai [162] also seems to be very popular among the nano-PCM works [21, 133, 140, 141]. The model measures the Brownian motion in terms of velocity and size of the particles. The Brownian motion enhanced thermal conductivity is then added into Maxwell's equation. The final equation is

$$k_{nf} = k_f \left[\frac{k_p + 2k_f + 2\varphi(k_p - k_f)}{k_p + 2k_f - \varphi(k_p - k_f)} \right] + C'\rho_{nf}c_{nf}|V|\varphi 2r_p \tag{15}$$

where V is the velocity and the constant C' can be empirically determined.

Particles clustering on effective thermal conductivity

Although various techniques are employed to produce stable nanofluids, problem of agglomeration cannot be

Table 7 Thermal conductivity models with effects of interfacial layers

Models	Formulations	Remarks
Yu and Choi [151]	$k_{nf} = k_f\left[\frac{k_{p,m}+2k_f+2\varphi(k_{p,m}-k_f)(1+\beta)^3}{k_{p,m}+2k_f-\varphi(k_{p,m}-k_f)(1+\beta)^3}\right]$ where $k_{p,m} = k_p\left[\frac{2(1-\gamma)+(1+\beta)^3(1+2\gamma)\gamma}{-(1-\gamma)+(1+\beta)^3(1+2\gamma)}\right]$	Modified Maxwell's model. Considers equivalent particle which is the combination of a particle and the nanolayer around it
Yu and Choi [152]	$k_{nf} = \left\{1+\frac{\left[\frac{1}{3}\sum_{j=a,b,c}(k_{pj}-k_f)/k_{pj}+(n-1)k_f\right]n\varphi_{eff}}{1-\left[\frac{1}{3}\sum_{j=a,b,c}(k_{pj}-k_f)/k_{pj}+(n-1)k_f\right]\varphi_{eff}}\right\}k_f$	Modified Hamilton–Crosser model. The particle–fluid interface is assumed as a confocal ellipsoid with a solid particle. Fails in predicting nonlinear variation
Xue [153]	$9(1-\varphi_T)\frac{k_{nf}-k_f}{2k_{nf}+k_f} + \varphi_T\left[\frac{k_{nf}-k_{cx}}{k_{nf}+B_{2x}(k_{cx}-k_{nf})} + 4\frac{k_{nf}-k_{cy}}{2k_{nf}+(1-B_{2x})(k_{cy}-k_{nf})}\right] = 0$ where φ_T–Total volume fraction of complex nanoparticles $= \frac{\varphi}{\lambda}$, $\lambda = \left(\frac{r_p}{r_p+t_v}\right)^3$	Based on average polarization theory. Introducing "complex nanoparticle" which is the particle with the interface between particle and liquid
Xue and Xu [154]	$(1-\varphi_T)\frac{k_{nf}-k_f}{2k_{nf}+k_f} + \varphi_T\left[\frac{(k_{nf}-k_l)(2k_l+k_p)-\lambda(k_p-k_l)(2k_l+k_{nf})}{(2k_{nf}+k_l)(2k_l+k_p)+2\lambda(k_p-k_l)(k_l-k_{nf})}\right] = 0$	Complex nanoparticle is considered to include the effect of interfacial layers
Xie et al. [155]	$\frac{k_{nf}-k_f}{k_f} = 3\Theta\varphi_T + \frac{3\Theta^2\varphi_T^2}{1-\Theta\varphi_T}$ where $\Theta = \frac{\left(\frac{k_l-k_f}{k_l+2k_f}\right)\left[\left(1+\frac{t_v}{r_p}\right)^3-\left(\left(\frac{k_p-k_l}{k_p+2k_l}\right)\left(\frac{k_f+2k_l}{k_f-k_l}\right)\right)\right]}{\left(1+\frac{t_v}{r_p}\right)^3+2\left[\left(\frac{k_l-k_f}{k_l+2k_f}\right)\left(\frac{k_p-k_l}{k_p+2k_l}\right)\right]}$	Employs equivalent hard sphere fluid model to consider microstructure of nanofluids

completely prevented. Agglomeration is nothing but getting together by the particles which is a result of van der Waals forces [164]. The clusters are generally porous in nature and occupy larger space than the individual particles [165]. Hence, it is expected to increase the effective thermal conductivity. Wang et al. [166] predicted the effective thermal conductivity using a model based on fractal theory (improved effective medium theory) in which the effect of nanoparticles clustering is considered. Although the model works good up to a volume fraction of less than 0.5%, the calculation is complicated. However, Wu et al. [167] who have also used a fractal model could not find any improvement in thermal conductivity due to particles clustering as the enhancement is dampened by reduced convection. Moreover, the effect of clustering on effective thermal conductivity is more pronounced only for higher concentrations [168, 169]. In case of nano-PCM composites, the higher concentrations are generally not preferred in order to keep natural convection in the liquid PCM intact. Even with lower concentrations, particles clustering can be alleviated using techniques like surface treatment by surfactants [81]. It is also observed from the literature on nano-PCM research that none of the works has made an attempt to include the particles clustering in evaluating effective thermal conductivity. From this perspective, the models with particles clustering effects are not deliberated in this review.

Viscosity models

As far as viscosity is concerned, the development of models for particles suspended liquids started way back in 1906 by Einstein [170]. This first wok came out with a linear equation which is

$$\mu_{nf} = \mu_f(1+2.5\varphi) \tag{16}$$

where μ_{nf} and μ_f are the dynamic viscosity of the nanofluid and the base fluid, respectively.

Table 8 Thermal conductivity models with effects of Brownian motion

Models	Formulations	Remarks
Koo and Kleinstreuer [161]	$k_{nf} = k_f\left[\frac{k_p + 2k_f + 2\varphi(k_p - k_f)}{k_p + 2k_f - \varphi(k_p - k_f)}\right] + 5 \times 10^4 \alpha\varphi\rho_f c_f f(T,\varphi)\sqrt{\frac{K_B T}{\rho_f 2r_p}}$	Takes into account the volume fraction of base fluid moving with a particle due to Brownian motion. Also considers the enhanced temperature dependence
Amiri and Vafai [162]	$k_{nf} = k_f\left[\frac{k_p+2k_f+2\varphi(k_p-k_f)}{k_p+2k_f-\varphi(k_p-k_f)}\right] + C'\rho_{nf}c_{nf}\lvert V\rvert\varphi 2r_p$	Enhancement due to Brownian motion is evaluated as a separate component and added into Maxwell component to obtain effective thermal conductivity. Brownian motion is accounted for by including velocity and size of the particles
Prasher et al. [157]	$k_{nf} = k_f\left(1 + 4 \times 10^4 \mathrm{Re}_B^m \overset{0.33}{\mathrm{Pr}}\ \varphi\right)\left[\frac{\{k_p(1+2Bi_p)+2k_m\}+2\varphi\{k_p(1-Bi)-k_m\}}{\{k_p(1+2Bi_p)+2k_m\}-\varphi\{k_p(1-Bi)-k_m\}}\right]$ where $m = 2.5$ $k_m = k_f(1 + 0.25 Re_B Pr)$, $Re_B = \frac{1}{\vartheta}\sqrt{\frac{18K_B T}{2\pi\rho_p r_p}}$, $Bi = \left(\frac{R_b k_m}{r_p}\right)$	Considers the effect of convection induced by Brownian motion of multiple particles. The effect of translational Brownian motion is negligible
Yang [158]	$k_{nf} = k_f\left[1 + 3\varphi\frac{\left(\frac{r_p}{R_b k_f}\right)-1}{\left(\frac{r_p}{R_b k_f}\right)+2}\right] + 157.5\varphi c_f\lvert V\rvert\tau$	Includes the microconvection which is a result of Brownian motion. Employs kinetic theory of particles and considers relaxation time of particles
Xuan et al. [159]	$k_{nf} = k_f\left[\frac{k_p+2k_f+2\varphi(k_p-k_f)}{k_p+2k_f-\varphi(k_p-k_f)} + \frac{\rho_p\varphi c_p}{2k_f}\sqrt{\frac{K_B T}{3\pi\mu r_c}}\right]$	The particle displacement is simulated according to theory of Brownian motion considering collision between particles, clusters or between particle and cluster. Fractal dimension is used to represent cluster structure
Jang and Choi [160]	$k_{nf} = k_f(1-\varphi_{eff}) + B_k k_p \varphi_{eff} + C_1 \frac{d_{bf}}{2r_p} k_f Re_{r_p}^2 \varphi_{eff}$ where $Re_{r_p} = \frac{2D_o r_p}{l_f \vartheta}$, $D_o = \frac{K_B T}{6\pi\mu r_p}$	Brownian motion is found to be inducing convection-like effects, whereas interaction between particles and fluid molecules promotes conduction heat transfer only. The model includes the relation between temperature/particle size and Brownian motion

This model was developed for rigid spherical particles and is applicable to non-interacting particles with a volume concentration of $\leq 2\%$.

Following Einstein [170], Brinkman [171] proposed a similar equation which is valid for volume fraction of up to 4%. Again this model is for only spherical, non-interacting particles. The model proposes the equation as

$$\mu_{nf} = \mu_f(1-\varphi)^{-2.5} \tag{17}$$

For higher concentrations, a model which is very similar to Eq. (17) is given by Roscoe [172]. But this model is limited to the cases wherein particles of equal size are used.

In the later years, Krieger and Dougherty [173], Frankel and Acrivos [174] and Neilsen [175] developed models in terms of maximum particle volume fraction (φ_{max}) at which the flow is still possible. The Krieger and Dougherty [173] model is expressed as

$$\mu_{nf} = \mu_f\left(1 - {}^{\varphi}/_{\varphi_{max}}\right)^{-\eta\varphi_{max}} \tag{18}$$

where η is the intrinsic viscosity which is taken as 2.5 for mono dispersed rigid, spherical particles. This means that this model may not be applicable to practical cases as mono dispersion of particles is difficult to come across. The model given by Frankel and Acrivos [174] is expressed as

$$\mu_{nf} = \mu_f \frac{9}{8}\left(\frac{(\varphi/\varphi_{max})^{1/3}}{1-(\varphi/\varphi_{max})^{1/3}}\right) \tag{19}$$

Similarly, Neilsen [175] recommended power law-based equation which is expressed as

Table 9 Viscosity models

Models	Formulations	Remarks
Einstein [170]	$\mu_{nf} = \mu_f(1 + 2.5\varphi)$	Valid for spherical, non-interacting particles with volume fraction of $\leq 2\%$
Brinkman [171]	$\mu_{nf} = \mu_f(1 - \varphi)^{-2.5}$	Valid for spherical, non-interacting particles with a volume fraction of up to 4%
Roscoe [172]	$\mu_{nf} = \mu_f(1 - 1.35\varphi)^{-2.5}$	Valid even for volume fraction of more than 4%, but for only equal size particles
Krieger and Dougherty [173]	$\mu_{nf} = \mu_f\left(1 - \varphi/\varphi_{max}\right)^{-\eta\varphi_{max}}$	Valid for mono dispersed rigid, spherical particles; practical applicability is limited
Frankel and Acrivos [174]	$\mu_{nf} = \mu_f \frac{9}{8}\left(\frac{(\varphi/\varphi_{max})^{1/3}}{1-(\varphi/\varphi_{max})^{1/3}}\right)$	Valid for uniform spherical particles of low volume fraction ($\leq 2\%$), related to maximum volume fraction
Neilsen [175]	$\mu_{nf} = \mu_f(1 + 1.5\varphi)e^{\varphi/(1 - \varphi_{max})}$	Power law-based expression, valid for volume fraction more than 2%
Batchelor [176]	$\mu_{nf} = \mu_f(1 + 2.5\varphi + 6.2\varphi^2)$	Includes the effect of hydrodynamic interactions between the particles, valid for volume fraction up to 10%
Lundgren [177]	$\mu_{nf} = \mu_f\left(1 + 2.5\varphi + \frac{25}{4}\varphi^2 + f(\varphi^3)\right)$	Expressed in the form of Taylor series, known as reduction of Einstein's model
Chen et al. [180]	$\mu_{nf} = \mu_f\left(1 - \frac{\varphi}{0.605}\left(\frac{r_c}{r_p}\right)^{1.2}\right)^{-1.5125}$	Takes into account the effect of particles agglomeration. New version of Krieger and Dougherty's model
Hosseini et al. [1]	$\mu_{nf} = \mu_f \exp\left[m + \alpha\left(\frac{T}{T_{ref}}\right) + \beta\varphi_h + \gamma\left(\frac{2r_p}{1-t_{cl}}\right)\right]$	Empirical model based on dimensionless groups. Includes the effect of particles interactions through hydrodynamic volume fraction
Corcione [181]	$\mu_{nf} = \mu_f\left(\frac{1}{1-34.87\left(r_p/r_f\right)^{-0.3}\varphi^{1.03}}\right)$ where r_f is the equivalent radius of a base fluid molecule which is given as $r_f = 0.05\left(\frac{6M}{1-N\pi\rho_{f,ref}}\right)^{1/3}$	Correlated using wide range of experimental data from the literature. Employed data of various combinations of nanomaterials and base fluids. Diameter of the particles ranging from 25 to 200 nm

$$\mu_{nf} = \mu_f(1 + 1.5\varphi)e^{\varphi/(1 - \varphi_{max})} \quad (20)$$

All the models discussed above have not considered the Brownian motion. However, Batchelor [176] has suggested a Brownian motion-based model as

$$\mu_{nf} = \mu_f\left(1 + 2.5\varphi + 6.2\varphi^2\right) \quad (21)$$

It is reported that the above model is valid for a volume fraction up to 10%. Another model which includes the Brownian motion is the one given by Lundgren [177]. The equation of the model is expressed in the form of Taylor series.

$$\mu_{nf} = \mu_f\left(1 + 2.5\varphi + \frac{25}{4}\varphi^2 + f\left(\varphi^3\right)\right) \quad (22)$$

Besides all these models, literature reveals some models expressed as empirical relations [178, 179]. The notable models are those proposed by Chen et al. [180], Hosseini et al. [1] and Corcione [181]. The viscosity models with the features are given in Table 9. For nano-PCM composites, the earlier works have majorly employed Brinkman model [133, 136, 137, 142, 182]. At the same time, Einstein model is also found a place in Faraji [182] and the one by Corcione [181] is used by Kashani et al. [140].

Latent heat models

It is generally believed that the there is a decrease in latent heat due to the volume occupied by the particles. Accordingly, all the numerical-based investigations have employed a straightforward expression to predict the latent heat of nano-PCM composites [20, 21, 30, 59, 61, 103, 136, 137, 140, 141]. The expression is written as

$$L_{\mathrm{nf}} = \frac{(1-\varphi)\rho_{\mathrm{f}} L_{\mathrm{f}}}{\rho_{\mathrm{nf}}} \tag{23}$$

It is clear that Eq. (23) is written only in terms of volume fraction of particles. As discussed in "Latent heat of composites" section, the size of the particles may have a role in affecting the latent heat of PCM. Further, there may be additional volume of PCM which cannot undergo phase change due to weak molecular bond structure. To the best of Authors' knowledge, none of the earlier works has considered the above while evaluating the latent heat of nano-PCM composites.

Conclusions

A review of literature concerning high-conductivity nanomaterials-added PCMs is presented. The effects of nanomaterials on thermo-physical properties of PCMs and subsequent effects on the thermal response are assessed. The models for evaluating the thermo-physical properties of nano-PCM composites are also discussed. The conclusions drawn out of this review are summarized below.

- Although the size of the nanoadditives should be as small as possible in order to avoid agglomeration, too smaller size may lead to reduction in thermal conductivity. This demands optimum size for thermal conductivity enhancement
- The size of the nanomaterial also has a role in latent heat reduction along with volume fraction
- The melting and solidification rates of PCMs cannot be increased linearly with increase in concentration of nanomaterials
- Rheology of nano-PCM composites still remains a least explored area and research on the same needs to be strengthened
- In PCM applications, the volume fraction of nanoadditives should be a trade-off between some important factors like, heat transfer enhancement, higher energy storage density, stability of nano-PCM, higher number of thermal cycles and cost saving.

Compliance with ethical standards

Conflict of interest The authors declare that they have no conflict of interest.

References

1. Hosseini SM, Moghadassi AR, Henneke DE. A new dimensionless group model for determining the viscosity of nanofluids. J Therm Anal Calorim. 2010;100(3):873–7.
2. Jegadheeswaran S, Pohekar SD. Performance enhancement in latent heat thermal storage system: a review. Renew Sustain Energy Rev. 2009;13(9):2225–44.
3. Tao YB, He YL. A review of phase change material and performance enhancement method for latent heat storage system. Renew Sustain Energy Rev. 2018;93:245–59.
4. Fan L, Khodadadi J. Thermal conductivity enhancement of phase change materials for thermal energy storage: a review. Renew Sustain Energy Rev. 2011;15:24–6.
5. Abdulateef AM, Mat S, Sopian K, Abdulateef J, Gitan AA. Experimental and computational study of melting phase-change material in a triplex tube heat exchanger with longitudinal/triangular fins. Sol Energy. 2017;155:142–53.
6. Sathish Kumar TR, Jegadheeswaran S, Chandramohan P. Performance investigation on fin type solar still with paraffin wax as energy storage media. J Therm Anal Calorim. 2019;136:101–12.
7. Li W, Wan H, Lou H, Fu Y, Qin F, He G. Enhanced thermal management with microencapsulated phase change material particles infiltrated in cellular metal foam. Energy. 2017;127:671–9.
8. Velraj R, Seeniraj RV, Hafner B, Faber C, Schwarzer K. Heat transfer enhancement in a latent heat storage system. Sol Energy. 1999;65:171–80.
9. Ettouney H, Alatiqi I, Al-Sahali M, Al-Hajirie K. Heat transfer enhancement in energy storage in spherical capsules filled with paraffin wax and metal beads. Energy Convers Manag. 2006;47(2):211–8.
10. Shiina Y, Inagaki T. Study on the efficiency of effective thermal conductivities on melting characteristics of latent heat storage capsules. Int J Heat Mass Transf. 2005;48(2):373–83.
11. Fan J, Wang L. Review of heat conduction in nanofluids. J Heat Transf. 2011;133(4):040801.
12. Wang X-Q, Mujumdar AS. Heat transfer characteristics of nanofluids: a review. Int J Therm Sci. 2007;46(1):1–19.
13. Mettawee E-BS, Assassa GMR. Thermal conductivity enhancement in a latent heat storage system. Sol Energy. 2007;81(7):839–45.
14. Chaichan MT, Kazem HA. Using aluminium powder with PCM (paraffin wax) to enhance single slope solar water distiller productivity in Baghdad—Iraq winter weathers. Int J Renew Energy Res. 2015;5:251–7.
15. Jegadheeswaran S, Pohekar SD, Kousksou T. Investigations on thermal storage systems containing micron-sized conducting particles dispersed in a phase change material. Mater Renew Sustain Energy. 2012;1(1):5.
16. Davarnejad R, Barati S, Kooshki M. CFD simulation of the effect of particle size on the nanofluids convective heat transfer in the developed region in a circular tube. Springerplus. 2013;2(1):192.
17. Lee J-H, Lee S-H, Choi C, Jang S, Choi S. A review of thermal conductivity data, mechanisms and models for nanofluids. Int J Micro-Nano Scale Transp. 2010;1(4):269–322.
18. Das SK, Choi SUS, Patel HE. Heat transfer in nanofluids—a review. Heat Transf Eng. 2006;27(10):3–19.
19. Kong L, Sun J, Bao Y. Preparation, characterization and tribological mechanism of nanofluids. RSC Adv. 2017;7(21):12599–609.
20. Fan L. Ph.D. Dissertation Thesis, Auburn University, Graduate Faculty; 2011.

21. Hosseinizadeh SF, Darzi AAR, Tan FL. Numerical investigations of unconstrained melting of nano-enhanced phase change material (NEPCM) inside a spherical container. Int J Therm Sci. 2012;51:77–83.
22. Michaelides EE. Brownian movement and thermophoresis of nanoparticles in liquids. Int J Heat Mass Transf. 2015;81:179–87.
23. Wei SK. Surface modification of silver nanoparticles in phase change materials for building energy application. Adv Mater Res. 2013;622–623:889–92.
24. Abolghasemi M, Keshavarz A, Mehrabian MA. Thermodynamic analysis of a thermal storage unit under the influence of nanoparticles added to the phase change material and/or the working fluid. Heat Mass Transf. 2012;48(11):1961–70.
25. Elbahjaoui R, El Qarnia H, El Ganaoui M. Melting of nanoparticle-enhanced phase change material inside an enclosure heated by laminar heat transfer fluid flow. Eur Phys J Appl Phys. 2016;74:24616.
26. Naeem LA, Al-Hattab TA, Abdulwahab MI. Study the performance of nano-enhanced phase change material NEPCM in packed bed thermal energy storage system. Int J Eng Trends Technol. 2016;37:72–9.
27. Manoj Kumar P, Mylsamy K. Experimental investigation of solar water heater integrated with a nanocomposite phase change material. J Therm Anal Calorim. 2019;136:121–32.
28. Lin SC, Al-Kayiem HH. Thermophysical properties of nanoparticles-phase change material compositions for thermal energy storage. Appl Mech Mater. 2012;233:127–31.
29. Zeng J-L, Zhu F-R, Yu S-B, Zhu L, Cao Z, Sun L-X, et al. Effects of copper nanowires on the properties of an organic phase change material. Sol Energy Mater Sol Cells. 2012;105:174–8.
30. Khodadadi JM, Hosseinizadeh SF. Nanoparticle-enhanced phase change materials (NEPCM) with great potential for improved thermal energy storage. Int Commun Heat Mass Transf. 2007;34(5):534–43.
31. Sebti SS, Mastiani M, Mirzaei H, Dadvand A, Kashani S, Hosseini SA. Numerical study of the melting of nano-enhanced phase change material in a square cavity. J Zhejiang Univ Sci A. 2013;14(5):307–16.
32. Constantinescu M, Dumitrache L, Constantinescu D, Anghel EM, Popa VT, Stoica A, et al. Latent heat nano composite building materials. Eur Polym J. 2010;46(12):2247–54.
33. Kalaiselvam S, Parameshwaran R, Harikrishnan S. Analytical and experimental investigations of nanoparticles embedded phase change materials for cooling application in modern buildings. Renew Energy. 2012;39(1):375–87.
34. Parameshwaran R, Jayavel R, Kalaiselvam S. Study on thermal properties of organic ester phase-change material embedded with silver nanoparticles. J Therm Anal Calorim. 2013;114:845–58.
35. Zeng JL, Sun LX, Xu F, Tan ZC, Zhang ZH, Zhang J, et al. Study of a PCM based energy storage system containing Ag nanoparticles. J Therm Anal Calorim. 2007;87:369–73.
36. Harikrishnan S, Kalaiselvam S. Preparation and thermal characteristics of CuO–oleic acid nanofluids as a phase change material. Thermochim Acta. 2012;533:46–55.
37. Jesumathy S, Udayakumar M, Suresh S. Experimental study of enhanced heat transfer by addition of CuO nanoparticle. Heat Mass Transf. 2012;48(6):965–78.
38. Ho CJ, Gao JY. Preparation and thermophysical properties of nanoparticle-in-paraffin emulsion as phase change material. Int Commun Heat Mass Transf. 2009;36:467–70.
39. He Q, Wang S, Tong M, Liu Y. Experimental study on thermophysical properties of nanofluids as phase-change material (PCM) in low temperature cool storage. Energy Convers Manag. 2012;64:199–205.
40. Teng TP, Yu CC. Characteristics of phase-change materials containing oxide nano-additives for thermal storage. Nanoscale Res Lett. 2012;7(1):611.
41. Raja Jeyaseelan T, Azhagesan N, Pethurajan V. Thermal characterization of $NaNO_3/KNO_3$ with different concentrations of Al_2O_3 and TiO_2 nanoparticles. J Therm Anal Calorim. 2019;136:235–42.
42. Kibria MA, Anisur MR, Mahfuz MH, Saidur R, Metselaar IHSC. A review on thermophysical properties of nanoparticle dispersed phase change materials. Energy Convers Manag. 2015;95:69–89.
43. Weinstein RD, Kopec TC, Fleischer AS, D'Addio E, Bessel CA. The experimental exploration of embedding phase change materials with graphite nanofibers for the thermal management of electronics. J Heat Transf. 2008;130:042405.
44. Shi JN, Der GM, Liu YM, Fan YC, Wen NT, Lin CK, et al. Improving the thermal conductivity and shape-stabilization of phase change materials using nanographite additives. Carbon N Y. 2013;51:365–72.
45. Kim S, Drzal LT. High latent heat storage and high thermal conductive phase change materials using exfoliated graphite nanoplatelets. Sol Energy Mater Sol Cells. 2009;93(1):136–42.
46. Jeon J, Jeong S-G, Lee J-H, Seo J, Kim S. High thermal performance composite PCMs loading xGnP for application to building using radiant floor heating system. Sol Energy Mater Sol Cells. 2012;101:51–6.
47. Li M. A nano-graphite/paraffin phase change material with high thermal conductivity. Appl Energy. 2013;106:25–30.
48. Elgafy A, Lafdi K. Effect of carbon nanofiber additives on thermal behavior of phase change materials. Carbon N Y. 2005;43(15):3067–74.
49. Sakalaukus PJ, Mosley A, Farah BI, Hsiao KT. Thermal conductivity characterization of nano-enhanced paraffin wax. In: Proceedings of the ASME international mechanical engineering congress & exposition. Colorado: ASME; 2011. p. 1753–1755.
50. Ryglowski BK. M.S. Dissertation Thesis, Naval Postgraduate School, Department of Mechnaical Engineering; 2009.
51. Yang DJ, Zhang Q, Chen G, Yoon SF, Ahn J, Wang SG, et al. Thermal conductivity of multiwalled carbon nanotubes. Phys Rev B. 2002;66(16):165440.
52. Kumaresan V, Velraj R, Das SK. The effect of carbon nanotubes in enhancing the thermal transport properties of PCM during solidification. Heat Mass Transf. 2012;48:1345–55.
53. Wang J, Xie H, Xin Z, Li Y, Chen L. Enhancing thermal conductivity of palmitic acid based phase change materials with carbon nanotubes as fillers. Sol Energy. 2010;84(2):339–44.
54. Lajvardi M, Zabihi F, Faraji H, Hadi I, Mollai J. The effect of phase change material on nanofluid heat transfer. In: Proceedings of the 4th international conference on nanostructures (ICNS4). Kish Island: Sharif University of Technology; 2012. p. 1176–78.
55. Ji P, Sun H, Zhong Y, Feng W. Improvement of the thermal conductivity of a phase change material by the functionalized carbon nanotubes. Chem Eng Sci. 2012;81:140–5.
56. Wu S, Ma X, Pen D, Bi Y. The phase change property of lauric acid confined in carbon nanotubes as nano-encapsulated phase change materials. J Therm Anal Calorim. 2018. https://doi.org/10.1007/s10973-018-7906-3.
57. Hasanabadi S, Sadrameli SM, Soheili H, Moharrami H, Heyhat MM. A cost-effective form-stable PCM composite with modified paraffin and expanded perlite for thermal energy storage in concrete. J Therm Anal Calorim. 2018. https://doi.org/10.1007/s10973-018-7731-8.

58. Selvaraj V, Morri B, Nair LM, Krishnan H. Experimental investigation on the thermophysical properties of beryllium oxide-based nanofluid and nano-enhanced phase change material. J Therm Anal Calorim. 2019. https://doi.org/10.1007/s10973-019-08042-w.
59. Arasu AV, Sasmito A, Mujumdar A. Numerical performance study of paraffin wax dispersed with alumina in a concentric pipe latent heat storage system. Therm Sci. 2013;17(2):419–30.
60. Arasu AV, Sasmito AP, Mujumdar AS. Thermal performance enhancement of paraffin wax with Al_2O_3 and CuO nanoparticles—a numerical study. Front Heat Mass Transf. 2011;2:043005.
61. Fan L, Khodadadi JM. An experimental investigation of enhanced thermal conductivity and expedited unidirectional freezing of cyclohexane-based nanoparticle suspensions utilized as nano-enhanced phase change materials (NePCM). Int J Therm Sci. 2012;62:120–6.
62. Fang X, Fan L-W, Ding Q, Yao X-L, Wu Y-Y, Hou J-F, et al. Thermal energy storage performance of paraffin-based composite phase change materials filled with hexagonal boron nitride nanosheets. Energy Convers Manag. 2014;80:103–9.
63. Harikrishnan S, Kalaiselvam S. Experimental investigation of solidification and melting characteristics of nanofluid as PCM for solar water heating systems. Int J Emerg Technol Adv Eng. 2013;3:628–35.
64. Motahar S, Nikkam N, Alemrajabi AA, Khodabandeh R, Toprak MS, Muhammed M. A novel phase change material containing mesoporous silica nanoparticles for thermal storage: a study on thermal conductivity and viscosity. Int Commun Heat Mass Transf. 2014;56:114–20.
65. Parlak M, Kurtuluş Ş, Temel ÜN, Yapici K. Thermal property investigation of multi walled carbon nanotubes (MWCNTs) embedded phase change materials (PCMs). In: Proceedings of 15th IEEE intersociety conference on thermal and thermomechanical phenomena in electronic systems (ITherm). Las Vegas: IEEE; 2016. p. 639–644.
66. Nabhan BJ. Using nanoparticles for enhance thermal conductivity of latent heat thermal energy storage. J Eng. 2015;21:37–51.
67. Teng TP, Yu CC. The effect on heating rate for phase change materials containing MWCNTs. Int J Chem Eng Appl. 2012;3(5):340–2.
68. Zabalegui A, Tong B, Lee H. Investigation of thermal properties in nanofluids for thermal energy storage applications. In: Proceedings of the ASME heat transfer summer conference. Minneapolis: ASME: V001T01A041-46; 2013.
69. Keblinski P, Eastman JA, Cahill DG. Nanofluids for thermal transport. Mater Today. 2005;8(6):36–44.
70. Eastman JA, Choi SUS, Li S, Yu W, Thompson LJ. Anomalously increased effective thermal conductivities of ethylene glycol-based nanofluids containing copper nanoparticles. Appl Phys Lett. 2001;78(6):718–20.
71. Masuda H, Ebata A, Teramae K, Hishinuma N. Alteration of thermal conductivity and viscosity of liquid by dispersing ultrafine particles. Netsu Bussei. 1993;7(4):227–33.
72. Lee S, Choi SU-S, Li S, Eastman JA. Measuring thermal conductivity of fluids containing oxide nanoparticles. J Heat Transf. 1999;121(2):280.
73. Temel UN, Kurtulus S, Parlak M, Yapici K. Size-dependent thermal properties of multi-walled carbon nanotubes embedded in phase change materials. J Therm Anal Calorim. 2018;132:631–41.
74. Haddad Z, Abu-Nada E, Oztop HF, Mataoui A. Natural convection in nanofluids: are the thermophoresis and Brownian motion effects significant in nanofluid heat transfer enhancement. Int J Therm Sci. 2012;57:152–62.
75. Murshed SMS, de Castro CAN. Contribution of Brownian motion in thermal conductivity of nanofluids. In: Ao SI, Gelman L, Hukins DWL, Hunter A, Korsunsky AM, editors. Proceedings of the World Congress on Engineering. London: Newswood Ltd; 2011. p. 1985–1989.
76. Chebbi R. Thermal conductivity of nanofluids: effect of brownian motion of nanoparticles. Am Inst Chem Eng J. 2015;61:2368–9.
77. Mahmoodi M, Kandelousi S. Effects of thermophoresis and Brownian motion on nanofluid heat transfer and entropy generation. J Mol Liq. 2015;211:15–24.
78. Azizian R, Doroodchi E, Moghtaderi B. Effect of nanoconvection caused by Brownian motion on the enhancement of thermal conductivity in nanofluids. Ind Eng Chem Res. 2012;51:1782–9.
79. Shukla RK, Dhir VK. Effect of Brownian motion on thermal conductivity of nanofluids. J Heat Transf. 2008;130(4):042406.
80. Prasher R, Bhattacharya P, Phelan PE. Brownian-motion-based convective-conductive model for the effective thermal conductivity of nanofluids. J Heat Transf. 2006;128:588–95.
81. Pirahmadian MH, Ebrahimi A. Theoretical investigation heat transfer mechanisms in nanofluids and the effects of clustering on thermal conductivity. Int J Biosci Biochem Bioinform. 2012;2(2):90–4.
82. Shin D, Banerjee D. Enhanced thermal properties of PCM based nanofluid for solar thermal energy storage. In: Proceedings of the ASME 4th international conference on energy sustainability. Phoenix: ASME; 2010. p. 841–845.
83. Prasher R, Song D, Wang J, Phelan P. Measurements of nanofluid viscosity and its implications for thermal applications. Appl Phys Lett. 2006;89(13):133108.
84. Zabalegui A, Lokapur D, Lee H. Nanofluid PCMs for thermal energy storage: latent heat reduction mechanisms and a numerical study of effective thermal storage performance. Int J Heat Mass Transf. 2014;78:1145–54.
85. Cai Y, Wei Q, Huang F, Lin S, Chen F, Gao W. Thermal stability, latent heat and flame retardant properties of the thermal energy storage phase change materials based on paraffin/high density polyethylene composites. Renew Energy. 2009;34(10):2117–23.
86. Saeed FR, Serban EC, Vasile E, Al-Timimi MHAA, Al-Banda WHA, Abdullah MZA, et al. Nanomagnetite enhanced paraffin for thermal energy storage applications. Dig J Nanomater Biostruct. 2017;12(2):273–80.
87. Teng T-P, Cheng C-M, Cheng C-P. Performance assessment of heat storage by phase change materials containing MWCNTs and graphite. Appl Therm Eng. 2013;50(1):637–44.
88. Xiang J, Drzal LT. Thermal conductivity of exfoliated graphite nanoplatelet paper. Carbon N Y. 2011;49(3):773–8.
89. Chieruzzi M, Cerritelli GF, Miliozzi A, Kenny JM. Effect of nanoparticles on heat capacity of nanofluids based on molten salts as PCM for thermal energy storage. Nanoscale Res Lett. 2013;8(1):448.
90. Risueño E, Gil A, Rodríguez-Aseguinolaza J, Gil A, Tello M, Faik A, et al. Thermal cycling testing of Zn–Mg–Al eutectic metal alloys as potential high-temperature phase change materials for latent heat storage. J Therm Anal Calorim. 2017;129:885–94.
91. Shaikh S, Lafdi K. A carbon nanotube-based composite for the thermal control of heat loads. Carbon N Y. 2012;50(2):542–50.
92. Zhang Y, Chen Z, Wang Q, Wu Q. Melting in an enclosure with discrete heating at a constant rate. Exp Therm Fluid Sci. 1993;6(2):196–201.
93. Ng KW, Gong ZX, Mujumdar AS. Heat transfer in free convection-dominated melting of a phase change material in a horizontal annulus. Int Commun Heat Mass Transf. 1998;25:631–40.

94. Tan FL. Constrained and unconstrained melting inside a sphere. Int Commun Heat Mass Transf. 2008;35(4):466–75.
95. Kole M, Dey TK. Effect of aggregation on the viscosity of copper oxide–gear oil nanofluids. Int J Therm Sci. 2011;50(9):1741–7.
96. Mahbubul IM, Saidur R, Amalina MA. Latest developments on the viscosity of nanofluids. Int J Heat Mass Transf. 2012;55(4):874–85.
97. Mostafavinia N, Eghvay S, Hassanzadeh A. Numerical analysis of melting of nano-enhanced phase change material (NePCM) in a cavity with different positions of two heat source-sink pairs. Indian J Sci Technol. 2015;8:49–61.
98. Mishra PC, Mukherjee S, Nayak SK, Panda A. A brief review on viscosity of nanofluids. Int Nano Lett. 2014;4(4):109–20.
99. Sridhara V, Satapathy LN. Al_2O_3-based nanofluids: a review. Nanoscale Res Lett. 2011;6(1):456.
100. Motahar S, Nikkam N, Alemrajabi AA, Khodabandeh R, Toprak MS, Muhammed M. Experimental investigation on thermal and rheological properties of *n*-octadecane with dispersed TiO_2 nanoparticles. Int Commun Heat Mass Transf. 2014;59:68–74.
101. Pak BC, Cho YI. Hydrodynamic and heat transfer study of dispersed fluids with submicron metallic oxide particle. Exp Heat Transf. 1998;11(2):151–70.
102. Xuan Y, Li Q. Heat transfer enhancement of nano-fluids. Int J Heat Fluid Flow. 2000;21:58–64.
103. Arasu AV, Mujumdar AS. Numerical study on melting of paraffin wax with Al_2O_3 in a square enclosure. Int Commun Heat Mass Transf. 2012;39(1):8–16.
104. Ho CJ, Gao JY. An experimental study on melting heat transfer of paraffin dispersed with Al_2O_3 nanoparticles in a vertical enclosure. Int J Heat Mass Transf. 2013;62:2–8.
105. Sciacovelli A, Colella F, Verda V. Melting of PCM in a thermal energy storage unit: numerical investigation and effect of nanoparticle enhancement. Int J Energy Res. 2013;37(13):1610–23.
106. Hosseini SMJ, Ranjbar AA, Sedighi K, Rahimi M. Melting of nanoprticle-enhanced phase change material inside shell and tube heat exchanger. J Eng. 2013;2013:784681.
107. Jourabian M, Farhadi M, Sedighi K. On the expedited melting of phase change material (PCM) through dispersion of nanoparticles in the thermal storage unit. Comput Math with Appl. 2014;67(7):1358–72.
108. Dhaidan NS, Khodadadi JM, Al-Hattab TA, Al-Mashat SM. Experimental and numerical investigation of melting of phase change material/nanoparticle suspensions in a square container subjected to a constant heat flux. Int J Heat Mass Transf. 2013;66:672–83.
109. Dhaidan NS, Khodadadi JM, Al-Hattab TA, Al-Mashat SM. Experimental and numerical investigation of melting of NePCM inside an annular container under a constant heat flux including the effect of eccentricity. Int J Heat Mass Transf. 2013;67:455–68.
110. Dhaidan NS, Khodadadi JM, Al-Hattab TA, Al-Mashat SM. Experimental and numerical study of constrained melting of *n*-octadecane with CuO nanoparticle dispersions in a horizontal cylindrical capsule subjected to a constant heat flux. Int J Heat Mass Transf. 2013;67:523–34.
111. Wu SY, Wang H, Xiao S, Zhu DS. An investigation of melting/freezing characteristics of nanoparticle-enhanced phase change materials. J Therm Anal Calorim. 2012;110(3):1127–31.
112. Patil P, Dey T. Experimental study of latent heat thermal energy storage system using PCM with effect of metal configurations and nano particles. Int J Curr Eng Technol. 2016;5:236–40.
113. Pise AT, Waghmare AV, Talandage VG. Heat transfer enhancement by using nanomaterial in phase change material for latent heat thermal energy storage system. Asian J Eng Appl Technol. 2013;2:52–7.
114. Hajare VS, Gawali BS. Experimental study of latent heat storage system using nano-mixed phase change material. Int J Eng Technol Manag Appl Sci. 2015;3:37–44.
115. Ebrahimi A, Dadvand A. Simulation of melting of a nano-enhanced phase change material (NePCM) in a square cavity with two heat source–sink pairs. Alex Eng J. 2015;54(4):1003–17.
116. Auriemma M, Iazzetta A. Numerical analysis of melting of parafn wax with Al_2O_3, ZnO and CuO nanoparticles in rectangular enclosure. Indian J Sci Technol. 2016. https://doi.org/10.17485/ijst/2016/v9i4/72601.
117. Murugan P, Ganesh Kumar P, Kumaresan V, Meikandan M, Malar Mohan K, Velraj R. Thermal energy storage behaviour of nanoparticle enhanced PCM during freezing and meltinge. Phase Transit. 2017;91:254–70.
118. Lokesh S, Murugan P, Sathishkumar A, Kumaresan V, Velraj R. Melting/solidification characteristics of paraffin based nanocomposite for thermal energy storage applications. Therm Sci. 2015;1:1–11.
119. Bashar MA. Ph.D. Dissertation Thesis, The University of Western Ontario, Department of Mechanical and Materials Engineering; 2016.
120. Esfe MH, Rejvani M, Karimpour R, Abbasian Arani AA. Estimation of thermal conductivity of ethylene glycol-based nanofluid with hybrid suspensions of SWCNT–Al_2O_3 nanoparticles by correlation and ANN methods using experimental data. J Therm Anal Calorim. 2017;128:1359–71.
121. El Omari K, Kousksou T, Le GY. Impact of shape of container on natural convection and melting inside enclosures used for passive cooling of electronic devices. Appl Therm Eng. 2011;31:3022–35.
122. Sun X, Zhang Q, Medina MA, Lee KO. On the natural convection enhancement of heat transfer during phase transition processes of solid-liquid phase change materials (PCMs). Energy Proc. 2014;61:2062–5.
123. Sun X, Zhang Q, Medina MA, Lee KO. Experimental observations on the heat transfer enhancement caused by natural convection during melting of solid–liquid phase change materials (PCMs). Appl Energy. 2016;162:1453–61.
124. Chandrasekaran P, Cheralathan M, Kumaresan V, Velraj R. Enhanced heat transfer characteristics of water based copper oxide nanofluid PCM (phase change material) in a spherical capsule during solidification for energy efficient cool thermal storage system. Energy. 2014;72:636–42.
125. Sebti SS, Khalilarya SH, Mirzaee I, Hosseinizadeh SF, Kashani S, Abdollahzadeh M. A numerical investigation of solidification in horizontal concentric annuli filled with nano-enhanced phase change material (NEPCM). World Appl Sci J. 2011;13:9–15.
126. Kashani S, Ranjbar AA, Abdollahzadeh M, Sebti S. Solidification of nano-enhanced phase change material (NEPCM) in a wavy cavity. Heat Mass Transf. 2012;48(7):1155–66.
127. Mahato A, Kumar D, Kumar A. Modelling of melting/solidification behaviour of nanoparticle-enhanced phase change materials. In: Proceedings of the 22nd National and 11th International ISHMT-ASME Heat and Mass Transfer Conference. Kharagpur: ASME; 2013.
128. Mahdi JM, Nsofor EC. Solidification enhancement in a triplex-tube latent heat energy storage system using nanoparticles-metal foam combination. Energy. 2017;126:501–12.
129. Hosseini M, Shirvani M, Azarmanesh A. Solidification of nano-enhanced phase change material (NEPCM) in an enclosure. J Math Comput Sci. 2014;8:21–7.
130. Sathishkumar A, Kathirkaman MD, Ponsankar S, Balasuthagar C. Experimental investigation on solidification behaviour of

water base nanofluid PCM for building cooling applications. Indian J Sci Technol. 2016;9(39):1–7.
131. Suresh Kumar KR, Kalaiselvam S. Experimental investigations on the thermophysical properties of CuO-palmitic acid phase change material for heating applications. J Therm Anal Calorim. 2017;129:1647–57.
132. Temirel M. M.S. Dissertation Thesis, Drexel University, Department of Mechnaical Engineering; 2015.
133. Sharma RK, Ganesan P. Solidification of nano-enhanced phase change materials (NEPCM) in a trapezoidal cavity: a CFD study. Univ J Mech Eng. 2014;2(6):187–92.
134. Sharma RK. Ph.D. Dissertation Thesis, University of Malaya, Faculty of Engineering; 2016.
135. El Hasadi YMF, Khodadadi JM. Numerical simulation of the effect of the size of suspensions on the solidification process of nanoparticle-enhanced phase change materials. J Heat Transf. 2013;135(5):052901.
136. Ali Rabienataj Darzi A, Farhadi M, Jourabian M, Vazifeshenas Y. Natural convection melting of NEPCM in a cavity with an obstacle using lattice Boltzmann method. Int J Numer Methods Heat Fluid Flow. 2013;24(1):221–36.
137. Ibrahem AM, El-Amin MF, Sun S. Effects of nanoparticles on melting process with phase-change using the lattice Boltzmann method. Results Phys. 2017;7:1676–82.
138. Sheikholeslami M. Numerical modeling of nano enhanced PCM solidification in an enclosure with metallic fin. J Mol Liq. 2018;259:424–38.
139. Sharifpur M, Yousefi S, Meyer JP. A new model for density of nanofluids including nanolayer. Int Commun Heat Mass Transf. 2016;78:168–74.
140. Kashani S, Lakzian E, Lakzian K, Mastiani M. Numerical analysis of melting of nanoenhanced phase change material in latent heat thermal energy storage system. Therm Sci. 2014;18(2):335–45.
141. Elbahjaoui R, El Qarnia H. Numerical analysis of melting of nano-enhanced phase change material in a rectangular latent heat storage unit. Int J Mech Mechatron Eng. 2016;10:1210–8.
142. Colla L, Ercole D, Fedele L, Mancin S, Manca O, Bobbo S. Nano-phase change materials for electronics cooling applications. J Heat Transf. 2017;139(5):052406.
143. Hosseini SS, Shahrjerdi A, Vazifeshenas Y. A review of relations for physical properties of nanofluids. Aust J Basic Appl Sci. 2011;5:417–35.
144. Wang BX, Zhou LP, Peng XF. Surface and size effects on the specific heat capacity of nanoparticles. Int J Thermophys. 2006;27(1):139–51.
145. Zhou LP, Wang BX, Peng XF, Du XZ, Yang YP. On the specific heat capacity of CuO nanofluid. Adv Mech Eng. 2010;2:172085.
146. Sharma KV, Suleiman A, Hassan Hj SB, Hegde G. Considerations on the thermophysical properties of nanofluids. In: Sharma KV, Hamid NHB, editors. Engineering applications of nanotechnology. Basel: Springer; 2017. p. 33–70.
147. Maxwell JC. A treatise on electricity and magnetism. 2nd ed. Cambridge: Oxford University Press; 1904.
148. Bruggeman DAG. The calculation of various physical constants of heterogeneous substances. I. The dielectric constants and conductivities of mixtures composed of isotropic substances. Ann Phys (Berlin). 1935;416:636–64.
149. Wang X-Q, Mujumdar AS. A review on nanofluids—part I: theoretical and numerical investigations. Braz J Chem Eng. 2008;25(4):613–30.
150. Hamilton RL, Crosser OK. Thermal conductivity of heterogeneous two-component systems. Ind Eng Chem Fundam. 1962;1(3):187–91.
151. Yu W, Choi SUS. The role of interfacial layers in the enhanced thermal conductivity of nanofluids: a renovated Maxwell model. J Nanoparticle Res. 2003;5(1/2):167–71.
152. Yu W, Choi SUS. The role of interfacial layers in the enhanced thermal conductivity of nanofluids: a renovated Hamilton–Crosser model. J Nanoparticle Res. 2004;6(4):355–61.
153. Xue QZ. Model for effective thermal conductivity of nanofluids. Phys Lett A. 2003;307(5–6):313–7.
154. Xue Q, Xu WM. A model of thermal conductivity of nanofluids with interfacial shells. Mater Chem Phys. 2005;90(2–3):298–301.
155. Xie H, Fujii M, Zhang X. Effect of interfacial nanolayer on the effective thermal conductivity of nanoparticle-fluid mixture. Int J Heat Mass Transf. 2005;48(14):2926–32.
156. Aybar HŞ, Sharifpur M, Azizian MR, Mehrabi M, Meyer JP. A review of thermal conductivity models for nanofluids. Heat Transf Eng. 2015;36(13):1085–110.
157. Prasher R, Phelan PE, Bhattacharya P. Effect of aggregation kinetics on the thermal conductivity of nanoscale colloidal solutions (nanofluid). Nano Lett. 2006;6(7):1529–34.
158. Yang B. Thermal conductivity equations based on Brownian motion in suspensions of nanoparticles (nanofluids). J Heat Transf. 2008;130:042408.
159. Xuan Y, Li Q, Hu W. Aggregation structure and thermal conductivity of nanofluids. AIChE J. 2003;49(4):1038–43.
160. Jang SP, Choi SUS. Role of Brownian motion in the enhanced thermal conductivity of nanofluids. Appl Phys Lett. 2004;84(21):4316–8.
161. Koo J, Kleinstreuer C. A new thermal conductivity model for nanofluids. J Nanoparticle Res. 2004;6(6):577–88.
162. Amiri A, Vafai K. Analysis of dispersion effects and non-thermal equilibrium, non-Darcian, variable porosity incompressible flow through porous media. Int J Heat Mass Transf. 1994;37(6):939–54.
163. Faraji M. Investigation of the melting coupled natural convection of nano phase change material: a fan less cooling of heat sources. Fluid Dyn Mater Process. 2017;13:19–36.
164. Wong KV, Castillo MJ. Heat transfer mechanisms and clustering in nanofluids. Adv Mech Eng. 2010;2:795478.
165. Gaganpreet, Sunitha S. Effect of aggregation on thermal conductivity and viscosity of nanofluids. Appl Nanosci. 2012;2(3):325–31.
166. Wang BX, Zhou LP, Peng XF. A fractal model for predicting the effective thermal conductivity of liquid with suspension of nanoparticles. Int J Heat Mass Transf. 2003;46(14):2665–72.
167. Wu C, Cho TJ, Xu J, Lee D, Yang B, Zachariah MR. Effect of nanoparticle clustering on the effective thermal conductivity of concentrated silica colloids. Phys Rev E. 2010;81(1):011406.
168. Feng Y, Yu B, Xu P, Zou M. The effective thermal conductivity of nanofluids based on the nanolayer and the aggregation of nanoparticles. J Phys D Appl Phys. 2007;40(10):3164–71.
169. Abbaspoursani K, Allahyari M, Rahmani M. An improved model for prediction of the effective thermal conductivity of nanofluids. Int J Mech Mechatronics Eng. 2011;5:1973–6.
170. Einstein A. Zur Theorie der Brownschen Bewegung. Ann Phys. 1906;324(2):371–81.
171. Brinkman HC. The viscosity of concentrated suspensions and solutions. J Chem Phys. 1952;20(4):571-571.
172. Roscoe R. The viscosity of suspensions of rigid spheres. Br J Appl Phys. 1952;3(8):267–9.
173. Krieger IM, Dougherty TJ. A mechanism for non-Newtonian flow in suspensions of rigid spheres. Trans Soc Rheol. 1959;3(1):137–52.
174. Frankel NA, Acrivos A. On the viscosity of a concentrated suspension of solid spheres. Chem Eng Sci. 1967;22(6):847–53.

175. Nielsen LE. Generalized equation for the elastic moduli of composite materials. J Appl Phys. 1970;41(11):4626–7.
176. Batchelor GK. The effect of Brownian motion on the bulk stress in a suspension of spherical particles. J Fluid Mech. 1977;83(01):97.
177. Lundgren TS. Slow flow through stationary random beds and suspensions of spheres. J Fluid Mech. 1972;51(02):273.
178. Alawi OA, Sidik NAC, Xian HW, Kean TH, Kazi SN. Thermal conductivity and viscosity models of metallic oxides nanofluids. Int J Heat Mass Transf. 2018;116:1314–25.
179. Meyer JP, Adio SA, Sharifpur M, Nwosu PN. The viscosity of nanofluids: a review of the theoretical, empirical, and numerical models. Heat Transf Eng. 2016;37(5):387–421.
180. Chen H, Ding Y, Tan C. Rheological behaviour of nanofluids. New J Phys. 2007;9(10):367.
181. Corcione M. Empirical correlating equations for predicting the effective thermal conductivity and dynamic viscosity of nanofluids. Energy Convers Manag. 2011;52(1):789–93.
182. Kean TH, Sidik NAC, Asako Y, Ken TL, Aid SR. Numerical study on heat transfer performance enhancement of phase change material by nanoparticles: a review. J Adv Res Fluid Mech Therm Sci. 2018;45:55–63.